HHS Public Access

Author manuscript

J Neuroimmune Pharmacol. Author manuscript; available in PMC 2017 March 01.

Published in final edited form as:

J Neuroimmune Pharmacol. 2016 March ; 11(1): 192–213. doi:10.1007/s11481-015-9645-6.

Δ9-tetrahydrocannabinol (Δ9-THC) promotes neuroimmune-modulatory microRNA profile in striatum of simian immunodeficiency virus (SIV)-infected macaques

Liz Simon[1,@], **Keijing Song**[2,@], **Curtis Vande Stouwe**[2,@], **Andrew Hollenbach**[3,@], **Angela Amedee**[4,@], **Mahesh Mohan**[5], **Peter Winsauer**[6,@], and **Patricia Molina**[1,*,@]

[1]Department of Physiology, Alcohol and Drug Abuse Center of Excellence

[2]Department of Physiology

[3]Department of Genetics, 533 Bolivar Street

[4]Department of Microbiology, Immunology, & Parasitology; Alcohol and Drug Abuse Center of Excellence

[5]Department of Comparative Pathology, Tulane National Primate Research Center, 18703 3 Rivers Rd, Covington, LA 70433

[6]Department of Pharmacology; Alcohol and Drug Abuse Center of Excellence

Abstract

Cannabinoid administration before and after simian immunodeficiency virus (SIV)-inoculation ameliorated disease progression and decreased inflammation in male rhesus macaques. Δ9-tetrahydrocannabinol (Δ9-THC) did not increase viral load in brain tissue or produce additive neuropsychological impairment in SIV-infected macaques. To determine if the neuroimmunomodulation of Δ9-THC involved differential microRNA (miR) expression, miR expression in the striatum of uninfected macaques receiving vehicle (VEH) or Δ9-THC (THC) and SIV-infected macaques administered either vehicle (VEH/SIV) or Δ9-THC (THC/SIV) was profiled using next generation deep sequencing. Among the 24 miRs that were differentially expressed among the four groups, 16 miRs were modulated by THC in the presence of SIV. These 16 miRs were classified into four categories and the biological processes enriched by the target genes determined. Our results indicate that Δ9-THC modulates miRs that regulate mRNAs of proteins involved in 1) neurotrophin signaling, 2) MAPK signaling, and 3) cell cycle and immune response thus promoting an overall neuroprotective environment in the striatum of SIV-infected macaques. This is also reflected by increased Brain Derived Neurotrophic Factor (BDNF) and decreased proinflammatory cytokine expression compared to the VEH/SIV group. Whether Δ9-THC-mediated modulation of epigenetic mechanisms provides neuroprotection in other regions of the brain and during chronic SIV-infection remains to be determined.

[*]Corresponding author: Patricia E. Molina, MD, Ph.D., Department of Physiology, LSUHSC, 1901 Perdido Street, Medical Education Building 7205, P7-3, New Orleans, LA 70112, Phone: 504-568-6187, Fax: 504-568-6158, pmolin@lsuhsc.edu.
[@]Louisiana State University Health Sciences Center, 1901 Perdido Street, New Orleans, LA 70112

Keywords

SIV; Cannabinoids; Striatum; miRNA

Introduction

Anti-retroviral therapy (ART) has increased the life span of persons living with Human Immunodeficiency Virus/Acquired Immunodeficiency Syndrome (PLWHA; HIV/AIDS), but it has concomitantly increased the incidence of HIV-associated neurocognitive dysfunction (HAND) (Antinori et al. 2007). Among the principal mechanisms proposed to mediate HIV dysregulation of brain function are chronic inflammation, glial cell activation, and neuronal injury (Gannon et al. 2011).

Cannabinoid use is frequent among PLWHA both recreationally and therapeutically (Molina et al. 2011a; SAMSHA 2005). Δ9-tetrahydrocannabinol (Δ9-THC; MARINOL® [dronabinol]) has been shown to improve appetite, weight gain, and overall quality of life among PLWHA (ElSohly et al. 2001). Previous studies from our laboratory have shown that chronic Δ9-THC administration before and during Simian Immunodeficiency Virus (SIV)-infection ameliorated disease progression, decreased early mortality from SIV, attenuated inflammation, and suppressed viral replication in male rhesus macaques (Molina et al. 2011b). Moreover, in these studies chronic Δ9-THC did not produce additive neuropsychological impairment to SIV infection. Macaques that received chronic Δ9-THC developed tolerance to its behaviorally disruptive effects, which was maintained for ~12 months of the study irrespective of SIV-infection. Postmortem histopathology data also indicated that chronic Δ9-THC reduced the frequency of brain pathology and opportunistic infections. These studies also showed that chronic Δ9-THC administration attenuated the expression of the proinflammatory cytokine, monocyte chemo attractive protein (MCP-1), and did not increase viral load in brain tissue or adversely affect markers of disease progression compared to vehicle-treated SIV-infected macaques (Winsauer et al. 2011). It is likely that Δ9-THC could modulate SIV disease progression by attenuating localized tissue inflammatory responses and viral replication (Ehrhart et al. 2005; Molina et al. 2011a).

In subsequent studies aimed at exploring the protective mechanisms involved in Δ9-THC-mediated amelioration of disease progression, we showed that chronic Δ9-THC produced changes in duodenal microRNA (miR) expression in SIV-infected macaques that were implicated in reducing inflammation and oxidative stress. These findings provide evidence that these protective effects may derive, in part, from Δ9-THC-dependent changes in the expression of miRs (Chandra et al. 2015; Molina et al. 2014). The functional consequences of alterations in miR are not yet fully understood. miRs play a critical role in the post-transcriptional regulation of gene expression in health and disease, are important in normal mammalian development, and regulate specific biological processes such as cell cycle, cell proliferation, apoptosis, immune response, and stem cell self-renewal and differentiation (Tsuchiya et al. 2006). In the brain, miRs are involved in neuronal development, cell differentiation, synapse formation and neuronal plasticity, and may be an underlying mechanism of cellular dysfunction contributing to diverse neurobehavioral deficits (Fiore

and Schratt 2007; Presutti et al. 2006). HIV infection has been shown to produce alterations in miR expression that may impact gene regulatory networks involved in HAND (Noorbakhsh et al. 2010; Tatro et al. 2010; Winkler et al. 2012). In addition, others have shown alterations in brain (Yelamanchili et al. 2010) and plasma miR profiles (Witwer et al. 2011) in SIV-infected macaques suggesting their involvement in modulation of disease progression.

The objective of the present study was to determine the effect of Δ9-THC on miR expression profile in the striatum of macaques during acute SIV-infection. The striatum was selected as a brain region of interest because the execution and maintenance of motor and cognitive commands are primarily dependent on its functional integrity (Nelson and Kreitzer 2014). Although HIV/SIV can infect any part of the brain, the striatum is particularly susceptible to increased viral replication and neuropathology leading to its marked atrophy in HIV-infected individuals (Meulendyke et al. 2014); (Sardar et al. 1996). Studies have also found decreased levels of several markers of neuronal integrity in the striatum of PLWHA and SIV-infected macaques, including N-acetyl aspartate. N-acetyl aspartate is a neuronal and axonal marker of integrity, predominantly found in the basal ganglia and frontal cortex, and is indicative of neuronal injury and inflammation (Anderson et al. 2015; Harezlak et al. 2011; Tracey et al. 1997). Although, the striatum is a major site of HIV/SIV replication in the brain, little is known about the effect of cannabinoids during acute HIV/SIV infection. Additionally, the role of cannabinoids in producing anti-inflammatory effects by modulating miR expression in the striatum is unknown.

In this study, using next generation sequencing (NGS) technology, we determined the normal miR expression profile in the striatum and its modulation by Δ9-THC during acute SIV infection of rhesus macaques. Our results showed that the major biological processes enriched with target genes are involved in immune response, neurotrophin signaling, tight junctions, regulation of transcription, and cell proliferation and apoptosis. We also detected increased BDNF expression and decreased mRNA expression of proinflammatory cytokines, in particular TNF-α, in the striatum of THC/SIV compared to VEH/SIV macaques. Thus, our results suggest that Δ9-THC-dependent changes in the expression of miR expression may contribute to protective neuromodulation in SIV-infected macaques.

Materials and Methods

Animal care, ethics and experimental procedures

All experiments using rhesus macaques were approved by the Tulane University and Louisiana State University Health Sciences Center (LSUHSC) Institutional Animal Care and Use Committees (Protocol No-3581) and adhered to the National Institutes of Health (NIH) guidelines for the care and use of experimental animals. The animals were housed in a Biosafety Level-2 containment building at Tulane National Primate Research Center. Animals were housed singly and provided a diet of monkey chow ad libitum (Lab Fiber Plus Primate diet DT; PMI Nutrition International, St. Louis, MO) supplemented with fruits, vitamins, and Noyes treats (Research Diets, New Brunswick, NJ).

Experimental design

Thirteen male Indian rhesus macaques three to seven years of age and with a body weight range of 5–11 kg were divided into four groups. Animals received two daily intramuscular injections of vehicle (1:1:18 of emulphor: alcohol: saline) or Δ9-THC. Chronic administration of Δ9-THC [or 0.05ml/kg VEH] was started four weeks before SIV infection at 0.18 mg/kg. Similar to previous studies, the dose was increased to 0.32 mg/kg over two weeks and continued for the entire duration of the study (Chandra et al. 2015; Molina et al. 2014). Vehicle-treated animals were further assigned to no infection (Group 1; VEH, n=2) or intravenous inoculation with 100_{TCID50} of SIVmac251 (Group 2; VEH/SIV, n=4). Δ9-THC-treated animals were further assigned to no infection (Group 3; THC, n=3) or SIV infection (Group 4; THC/SIV, n=4). All animals were euthanized at 60 days post-SIV infection, a time when all animals were asymptomatic. Tissue samples including the brain were collected at necropsy, flash frozen, and stored at −80 °C. The animals were not perfused prior to sample collection. The impact of chronic THC administration on SIV-induced alterations in intestinal microRNA profiles in this cohort of animals has been reported elsewhere (Chandra et al. 2015).

Brain viral load

SIV RNA levels in plasma and striatum of the brain were determined by qPCR as previously published (Chandra et al. 2015; Molina et al. 2014). For tissue SIV levels, total RNA was extracted from flash frozen striatum using Trizol reagent (Life Technologies, Grand Island, NY) according to the manufacturer's instructions. SIV RNA levels were quantified by adding approximately 100 ng of sample RNA to duplicate qPCR amplification assays. The average SIV RNA copy number was determined and normalized to micrograms of RNA utilizing a qPCR assay that targets the housekeeping gene, RPS13, with validated Taqman primers and probe as described (Clark-Langone et al. 2007). The limit of detection in these assays is 50 copies SIV RNA per microgram RNA. Samples with undetectable levels of SIV were assigned a value of 25, and all values were log10-transformed for comparisons of treatment groups.

RNA isolation and deep sequencing

Deep sequencing was performed on the striatum of two macaques from each treatment group. The results obtained from deep sequencing were then confirmed using qPCR on all the animals in the treatment groups. RNA was isolated from striatum using an RNA isolation kit (Norgen, Ontario, Canada) according to the manufacturer's protocol and the concentrations measured using a Nanodrop. The RNA was then sent to LC Biosciences (Houston, TX) for preparation of the small RNA sequencing library and deep sequencing. Briefly; a small RNA library was generated using Illumina Truseq™ Small RNA Preparation kit. The purified cDNA library was used for cluster generation on Illumina's Cluster Station and sequenced on Illumina GAIIx. Raw sequencing reads (40 nts) were obtained using Illumina's Sequencing Control Studio software version 2.8 (SCS v2.8) following real-time sequencing image analysis and base-calling by Illumina's Real-Time Analysis version 1.8.70 (RTA v1.8.70). A proprietary pipeline script, ACGT101-miR v4.2 (LC Sciences), was used for sequencing data analysis.

Sequencing data analysis and normalization

Sequencing data analysis and normalization was performed by LC Biosciences on 2 animals from each group. The results provided were used in the selection of specific miRs to be validated by PCR. After Sequenced Sequences (sequ seqs) were extracted, digital filters (LC Sciences) were employed to remove un-mappable sequencing reads by generating unique families of Sequ Seqs by sorting raw sequencing reads and filtering Sequ Seqs. The mapped reads were then identified against pre-miR (mir) and mature miR (miR) sequences listed in miRBase 5, 6, 7 or genome based on the public releases of appropriate species. For normalization of read counts in each sample, the counts were divided by a library size parameter (median value of the ratio between the counts of a specific sample and a pseudo-reference sample) of the corresponding sample. A count number in the pseudo-reference sample is the count geometric mean across all samples. The data set normalized against the miRs was used for subsequent analysis. The miR reads that were significantly different ($p<0.05$) between the four groups were determined using ANOVA. A total of 26 miRs were significantly different between the groups (Supplemental table 1). Among these, eight miRs had similar level of expression in SIV, THC/SIV and THC groups and thus, were not used for further analysis. The miR reads that were significantly different between the two treatment groups (THC/SIV and VEH/SIV) were determined by a t-test and used for further analysis. The validated targets of differentially expressed miRs were determined using miRTarbase and TargetScan was used to determine predicted and validated gene targets of differentially expressed miRs. TargetScan is the most advanced, widely used, and relatively conservative database. The biological processes of the predicted or validated targets were determined using GeneCodis (Carmona-Saez et al. 2007; Nogales-Cadenas et al. 2009; Tabas-Madrid et al. 2012) and gene enriched KEGG pathways were determined using Database for Annotation, Visualization and Integrated Discovery (DAVID) (Huang da et al. 2009a; Huang da et al. 2009b).

Quantitative real-time PCR (qPCR) for miR expression

To validate the deep sequencing data, the relative expression of three differentially expressed miRs (miR-7, miR-181a, miR-27b) was further determined by individual Taqman miR assays in all the animals in the VEH/SIV (n=4) and THC/SIV (n=4) groups. Approximately 200–250 ng of total RNA was reverse-transcribed using the stem loop primers provided in the predesigned kit and ~1.3 μl of cDNA was subjected to 40 cycles of PCR on the CFX96 Bio-Rad PCR cycler (Bio-Rad) using the following thermal cycling conditions: 50°C for two minutes, 95°C for ten minutes followed by 40 repetitive cycles of 95°C for 15 seconds and 60°C for one minute. As a normalization control for RNA loading, RNU48 and SNOU6 were amplified in duplicate wells on the same multi-well plate.

qPCR for target genes of differentially regulated miRNAs

Total RNA isolated for miR sequencing studies was used for gene expression analysis as well. cDNA was synthesized from 500 ng of the resulting total RNA using the Quantitect Reverse Transcriptase Kit (Qiagen), in accordance with the manufacturer's instructions. Primers were designed to span exon-exon junctions (IDT, Coralville, IA) and used at a concentration of 500 nmol. The final reactions were made to a total volume of 20 μl with

Quantitect SyBr Green PCR kit (Qiagen). All reactions were carried out in duplicate on a CFX96 system (Bio-Rad Laboratories, Hercules, CA) for quantitative real-time PCR (qPCR) detection. qPCR data were analyzed using the comparative Ct (delta-delta-Ct, ΔΔCT) method. Target genes were compared with the endogenous control, ribosomal protein S13 (*RPS13*), and THC/SIV values were normalized to VEH/SIV values.

Western blot analysis for BDNF

Striatal samples from all animals in the treatment groups (VEH n=2, VEH/SIV n=4, THC/SIV n=4) were homogenized in T-PER (Pierce Thermo Scientific, Rockford, IL) buffer with Halt protease and phosphatase inhibitor cocktail (Thermo Scientific). Samples were centrifuged at 10,000 g for five minutes at 4°C, and protein concentrations determined by the BCA protein assay kit (Thermo Fisher Scientific). Equal amounts of protein (50ug) were separated by Tris-tricine 10–20% Mini-protein gels (Bio-Rad) and transferred to Immobilon-P^{SQ} transfer membrane (Millipore, Billerica, MA). Rabbit polyclonal anti-human BDNF (Santa Cruz Biotechnology, Santa Cruz, CA USA) at a final concentration of 1:200 was used for protein expression analysis. Bands were visualized using ECL chemiluminescence kit (Millipore, Billerica, MA, USA) and densitometric analysis performed using ImageJ software. An internal control, HRP-conjugated β-Actin (Santa Cruz Biotechnology, Santa Cruz, CA. USA) was used as the loading control. The band densities were analyzed using One-Way Analysis of Variance.

Results

Viral loads in plasma and brain

No significant differences in mean plasma viral loads at the time of necropsy (60 days post-SIV) were detected between the VEH/SIV and THC/SIV macaques. Similarly, SIV RNA levels in the striatum were not different between the groups (mean±SEM log viral loads of 2.00±0.29 and 2.27±0.19 SIV copies/μg RNA in VEH/SIV and THC/SIV animals, respectively).

miR sequencing and annotations

miR profiling of the striatum from the four treatment groups was performed using the Illumina small RNA TrueSeq kit and sequenced on Illumina GAIIx. The length of the detected sequences varied between 15 and 45 nucleotides and 50.1% were between 19–23 nucleotides. The frequency of reads mapping to mature miRs had a median of 52.5%. In addition, a fraction of reads were mapped to snRNA, miscRNA, tRNA, rRNA, and mRNA. The sequencing data was deposited in GEO repository database (http://www.ncbi.nlm.nih.gov/geo/), which is retrievable under the accession number (GSE72766).

Profiling of miRs differentially regulated between the treatment groups

The miRs that were differentially regulated among the four different treatment groups (VEH, VEH/SIV, THC and THC/SIV) were divided into four categories based on criteria defined below. The miR expression in the four categories were 1.5-fold greater or less than that of VEH. Figure 1 shows the graphical representation of miR fold-change in the respective different categories. Validated (miRTarbase) or predicted targets (top 200 genes

with a context score of −0.3 or lower, TargetScan) were used to identify biological processes (BP) of enriched target genes in each category using GeneCodis (p>0.0001).

Category 1 included miRs whose expression was significantly increased (≥1.5 fold) only in the presence of both SIV and THC (THC/SIV group). The target genes for miRs (Table 1) in this category were enriched in major BPs including DNA repair, negative regulation of apoptosis and viral reproduction, and response to stress. There were also genes enriched in brain development and synaptic transmission in this category (Table 5). Out of the ten miRNAs in this category, five of them (miR-485, -382, -134, -381 and -539) are clustered miRNAs positioned within 10 kb of each other and located on chromosome 7 in Rhesus and chromosome 14 in humans (miRBase). An examination of the UCSC Genome Browser on Human (Feb. 2009) (http://genome.ucsc.edu/) (Kent et al. 2002) demonstrated that this region on the chromosome is enriched for H3K227Ac histone mark, which indicates a region of enhanced transcriptional activity. The transcription factors that have been identified to bind to these regions of the chromosome are Fos, Jun, FoxA1, Foxa2, Sp1 and GATA.

Category 2 included miRs that showed significant decrease in expression during SIV infection or in the presence of THC alone but that were maintained at control levels in the THC/SIV group. The target genes for miRs (Table 2) in this category were enriched in major BPs such as regulation of transcription and cell migration, FGF signaling pathway, and axon guidance (Table 5). KEGG pathway analysis of target genes revealed that gene enrichment was the most significant for axon guidance, tight junction and MAPK signaling.

Category 3 included miRs that were significantly decreased during SIV infection or THC alone but whose expression was significantly increased in the THC/SIV relative to the VEH group. The target genes in this category (Table 3) were enriched in BPs such as immune response, toll like receptor pathway, the negative regulation of apoptotic process, and cell proliferation (Table 5).

Category 4 included miRs that showed a significant decrease in expression in the presence of both SIV and THC relative to all other groups. Both the miRs in this category were in a single cluster located on Chromosome 15 in rhesus macaques and chromosome nine in humans as demonstrated by the UCSC Genome Browser on Human (February 2009). The transcription factors that have been identified to bind to these regions of the chromosome are ESR1, CTCF and PolR2a. The target genes in this category (Table 4) were enriched in BPs such as negative regulation of apoptosis and cell proliferation, regulation of transcription, and insulin receptor signaling pathway (Table 5).

The miRs that were differentially expressed between VEH/SIV and THC/SIV groups alone were also analyzed. Six miRs were found to be significantly up and downregulated between the two groups respectively (Table 6). The major BPs enriched by target mRNAs of miRs that were upregulated in the THC/SIV group included regulation of transcription, apoptosis, positive regulation of cell proliferation and chromatin modification. The target genes of miRs that were downregulated in the THC/SIV compared to the VEH/SIV group were enriched in BPs such as regulation of transcription, nerve growth factor signaling pathway,

cell cycle, MAPK cascade, response to hypoxia, and insulin receptor signaling pathway (Table 7). The KEGG pathway with the most significant gene-enrichment of upregulated miRs was integrin signaling and that for the down-regulated miRs were MAPK signaling, tight junctions, endocytosis and neurotrophin signaling.

Confirmation (qPCR and target gene expression) of select differentially regulated miRs

The expression of a select list of differentially expressed miRs (miR-7, miR-181a and miR-27b) was confirmed by qPCR (Fig. 2). The qPCR results confirmed a similar expression pattern observed with the deep sequencing reads for all three miRs, but did not reach statistical significance.

Two miRs (miR-134, and -151) that were differentially regulated in the deep sequencing analysis target brain derived neurotrophic factor (BDNF), an important modulator of neuronal survival. Relative expression as determined by qPCR of miR-134 was 1.00±0.2 and 2.77±0.88 and that of miR-151b 1.00±0.12 and 1.09±0.37 in the striatum of VEH/SIV and THC/SIV macaques respectively, failing to confirm the findings from the deep sequencing analysis. However, mRNA expression of BDNF in the striatum was found to be decreased by approximately 97% in VEH/SIV as compared to the VEH group and threefold higher in the THC/SIV group compared to that in the VEH/SIV group (Fig 3). Moreover, Western blot analysis of BDNF detected two major bands, 28kDa and 14 kDa and a statistically significantly greater expression of the 28 kDa band and a trend to increased expression of the 14 kDa band in THC/SIV compared to VEH/SIV striatum. Taken together, these results suggest functional relevance of the findings from the deep sequencing analysis, despite the lack of corroboration with qPCR of the differences in miR-134 and miR-151 expression.

mRNA expression of proinflammatory cytokines mRNA expression of TNF-α was significantly lower in the striatum of THC/SIV compared to that of the VEH/SIV group. mRNA expression of other cytokines such as IL-6, IL-1B, MCP-1 was also decreased compared to that of VEH/SIV animals, but this difference failed to reach statistical significance (Fig 4).

Discussion

This study investigated the impact of chronic THC administration on striatal miR expression in SIV-infected macaques. We explored the possibility that changes in miR expression profile may contribute to the protective modulation of neurobiological functions. We identified a number of miRs that were differentially expressed in the striatum of THC-treated SIV-infected macaques. Our results showed that the major biological processes enriched with target genes are involved in immune response, neurotrophin signaling, tight junctions, regulation of transcription, and cell proliferation and apoptosis. We also demonstrated an increase in striatal BDNF and a decrease in TNF-α mRNA expression in THC/SIV compared to VEH/SIV group. These findings provide evidence to support the prediction that Δ9-THC-dependent modulation of miR expression may be a mechanism underlying the neuroprotective effects of THC. The neuroprotective effects may part be mediated by altering neuroinflammation and neurotrophin signaling.

Previous studies from our laboratory demonstrated that chronic Δ9-THC reduced brain pathology, decreased proinflammatory cytokine expression, and decreased viral load in brain tissue without producing additive neuropsychological impairment in SIV-infected male macaques (Winsauer et al. 2011). Subsequently, in a different cohort of animals, we demonstrated a role for differential miR expression in Δ9-THC-mediated suppression of intestinal inflammation in acute-SIV infection (Chandra et al. 2015). However, to date, data linking these two observations has been lacking. The results from the present study establish this link and provide supporting evidence for post-transcriptional epigenetic modifications as part of the underlying mechanism of THC-mediated neuroprotection in SIV-infected macaques.

It is interesting to note that five out of the ten differentially expressed miRs in category 1 (THC/SIV has a significant increase in miR expression) were part of a single cluster, mir-379/mir-656 (Glazov et al. 2008) or C14 miRs (Laddha et al. 2013), that is expressed highly in brain and placental samples. Similarly, both miRs in category 4 (THC/SIV decreases miR expression) were part of another cluster. miRs are classified to be in a cluster if the pairwise chromosomal distances are at most 3000 nucleotides (Altuvia et al. 2005) or within a distance of 10 kb (miRBase). Expression of clustered miRs are believed to be similar if located on the same polycistronic transcripts and may coordinate an intricate regulatory network (Chan and Lin 2015). Although the functional relevance of miR clusters are still unknown, they may function more efficiently as a miR-mediated network than through individual miRNA mediated modulation of gene expression alone (Zhang et al. 2009). Our results suggest that Δ9-THC might be regulating miR clusters that then coordinately regulate multiple biological processes such as cell cycle, cell differentiation, and neuroinflammation.

The gene enriched pathways for the two miRs that showed similar levels of expression in the THC/SIV and VEH groups and at the same time were decreased in the VEH/SIV group (Category 2) were axon guidance, MAPK and tight junction maintenance and function. Axon guidance recruits specific paths and defines their termination zones and synaptic partners (Cho et al. 2014; Lim et al. 2008), and is required for the development, maintenance, and plasticity of neural circuits (Curinga and Smith 2008). Axon guidance is relevant in adult life in response to injury. The adult regenerating axons, unlike the developing neurons, are in an adverse milieu that has reactive immune cells and astrocytes, cytokines, extracellular matrix (ECM) components, and reactive oxygen species, which could change the direction of the growth cone (Curinga and Smith 2008). HIV gp120 has become known to promote axonal degeneration (Melli et al. 2006) and axon damage is one of the predictors of HIV-associated neurocognitive disorders (HAND). Genes involved in the axon guidance pathway have been shown to be downregulated in the frontal cortex of HIV-associated dementia (HAD) patients compared to patients without dementia (Zhou et al. 2012). Activation of MAPK has been shown to be necessary for the establishment of normal neural connectivity patterns within the brain (Soundararajan et al. 2010). Several genes involved in the MAPK pathway has been shown to be significantly reduced in the frontal cortex of patients with HAD compared to non-dementia patients (Zhou et al. 2012). The MAPK pathway also plays a crucial role in HIV replication and virulence (Yang and Gabuzda 1999) and communicates with the JAK-STAT signaling pathway, an important

mediator of growth factor and cytokine signaling that plays a key role in cell proliferation, differentiation, migration and apoptosis (Zhou et al. 2012).

In a retrospective study using the frontal cortex of patients with and without HAD (Zhou et al. 2012), miR-137 was found to be significantly down regulated in patients with HAD. miR-137 is enriched in neurons (Smrt et al. 2010) and modulates neuronal cell proliferation and differentiation (Smrt et al. 2010; Szulwach et al. 2010). Zhou et al. previously demonstrated that miR-137 can target more than 5 neurodegeneration related pathways in patients with HAD (Zhou et al. 2012). Although no significant histopathological changes were noted in the brains used for analysis in this study (data not shown), our results showed increased miR-137 expression in the striatum of THC/SIV compared to VEH/SIV group. The increase in miR-137 in the THC/SIV group may potentially be a compensatory mechanism involved in downregulation of genes involved in neurodegeneration pathways, thus providing neuroprotection to the striatum.

The pathways that were enriched for target genes of miRs that were downregulated in the THC/SIV group compared to the VEH/SIV group alone included MAPK signaling (already discussed), tight junctions, endocytosis and neurotrophin signaling. Endocytosis is a critical aspect of neurotrophin signaling, axon and dendrite growth and signaling, and efficient internalization of the signaling complex (Bashaw and Klein 2010; Cosker and Segal 2014). Endocytotic trafficking defects have been described in neurodegenerative disorders such as Alzheimer's disease (Choi et al. 2013). At least 7 predicted target genes represented critical components of the endocytosis pathway, suggesting that THC may play a role in modulating the endocytotic pathway and neurotrophin signaling.

The neurotrophin family of growth factors includes BDNF, nerve growth factor (NGF) and neurotrophins 3 and 4/5. BDNF is known to support neuronal survival, growth and differentiation (Chao et al. 2011; Chao and Lee 2004) and has been suggested to be neuroprotective against HIV-mediated cell injury (Bachis et al. 2003; Mocchetti and Bachis 2004) as reflected by the BDNF-mediated reduction in caspase-3 mediated activation of apoptosis both in vivo and in vitro. (Bachis et al. 2012; Bachis et al. 2003; Sanders et al. 2000). In addition, both NGF and BDNF have been shown to promote neuronal survival in HIV infection by inducing expression of the anti-apoptotic gene, Bcl-2 (Ramirez et al. 2001). We detected a 95% decrease in BDNF mRNA expression in VEH/SIV compared to VEH, and three-fold higher expression of BDNF in the THC/SIV ($p=0.07$) compared to the VEH/SIV group. Western blotting for BDNF detected 2 major bands: 14 kDa and 28 kDa. A significant increase in the expression of 28 kDa was seen in the THC/SIV compared to VEH/SIV group. In addition, a trend for an increase in the expression of the 14 kDa band was also noted in the THC/SIV striatum. The molecular weight of pro-BDNF is 32kDa, the 28 kDa band is a truncated form of pro-BDNF and 14 kDa band, the mature form (Garcia et al. 2012; Mowla et al. 2001). Although the biological functions of the truncated form are not known, it was recently demonstrated that the expression of the truncated form was reduced in schizophrenic patients (Carlino et al. 2011) and in autism (Garcia et al. 2012). Thus our data suggests that THC may be modulating neurotrophin signaling to provide neuroprotection.

Among the upregulated miRs in striatum of THC/SIV compared to that of VEH/SIV group, target genes of several miRs were enriched for integrin signaling, including genes such as collagen type III α1, laminin γ2 and 3, and integrin α5. The HIV Tat protein produces increased focal adhesion through integrin signaling, thus promoting cell migration and increasing blood brain barrier (BBB) permeability (Avraham et al. 2004; Berrier and Yamada 2007). THC-mediated upregulation of miRs involved in integrin signaling may decrease the expression of genes that promote endothelial cell migration and increased BBB permeability. HIV invades the brain by migration of infected leukocytes across the BBB (Buckner et al. 2008), promoting an inflammatory response involving immune cell infiltration and microglial cell activation, which more strongly correlates with the degree of neurological impairment than viral load levels (Fraga et al. 2011; Glass et al. 1993). In vitro studies have shown that HIV Tat protein promotes adhesion of U937 cells to ECM proteins and this is prevented by Δ9-THC. Cells that were exposed to Δ9-THC had fewer projections into the ECM resulting in cytoskeletal reorientation and reduced cell transmigration (Berrier and Yamada 2007). We speculate that a potential mechanism of Δ9-THC-mediated neuroprotection in the striatum may result from reduced integrin-ECM interaction and signaling.

A limited number of studies have performed large-scale miR profiling of HIV/SIV-infected brains. In a comprehensive miR profiling study that was performed on the caudate and hippocampus of uninfected and SIV-infected macaques (Yelamanchili et al. 2010), six miRs were significantly upregulated in the caudate, and four in the hippocampus of macaques with encephalitis. miR profiling performed on the frontal cortex of patients with HAD or HIVE (Noorbakhsh et al. 2010; Tatro et al. 2010; Zhou et al. 2012) demonstrated several differentially expressed miRs of which some miRs showed similar expression patterns in the present study. For example, miR-137 was significantly downregulated in the brains of HAD patients (Zhou et al. 2012) and showed increased expression in the THC/SIV group in our study. miR-21, miR-142-5p, and miR-142-3p that were upregulated in human and macaque HIV/SIV studies (Noorbakhsh et al. 2010; Yelamanchili et al. 2010) but were not differentially expressed in the current study. The discrepancy might be due to the area of the brain profiled and the stage of infection.

Several of the miRs shown to be differentially expressed in striatum of THC/SIV vs. VEH/SIV animals, including miR-181a and miR-7, target genes with immunomodulatory function. In particular, miR-7, of which downregulation has been shown to promote an inflammatory response (Kong et al. 2012), was significantly increased in striatum of THC/SIV compared to VEH/SIV and VEH animals (Category 3), and had the highest number of reads among all differentially expressed miRs. Previously we have reported that chronic Δ9-THC administration decreased inflammation in the duodenum and brain of SIV-infected macaques (Chandra et al. 2015; Molina et al. 2011a; Molina et al. 2014; Winsauer et al. 2011), suggesting that the protective effects of Δ9-THC are directly linked to its immunomodulatory actions. The brain is an early target of HIV infection and the pathology has been proposed to be primarily mediated by neuroinflammation (Hurtrel et al. 1991). Consistent with this finding, recently published studies have demonstrated that Δ9-THC-induced immunomodulation may directly reduce SIV/HIV neuropathogenesis (Cabral and Griffin-Thomas 2008). Our results provide additional strong evidence of the significant

immunomodulatory effects of -9THC as reflected by attenuation of proinflammatory gene expression including TNF-α, MCP-1, IL-1B and IL-6 in the THC/SIV compared to the VEH/SIV group. gp120 and TNF-α are commonly upregulated in HIVE, reduce intracellular stores and transport of BDNF, stimulate NMDA receptors (Bachis et al. 2003), and reduce hippocampal neurogenesis (Hasler 2010; Raedler 2011). Selective stimulation of cannabinoid type-2 receptors (CB2) has been reported to decrease CD40 expression and microglial TNF-α production (Ehrhart et al. 2005). Thus, taken together these results suggest that chronic Δ9-THC modulates neuroinflammation by attenuating pro-inflammatory cytokine expression and enhancing BDNF expression, which we speculate confers neuroprotection through decreased neuroinflammation and neurodegeneration.

In summary, our results show that Δ9-THC modulates miRs that modulate neurotrophin and MAPK signaling, cell cycle, and neuroinflammation, which together confer neuroprotection of the striatum during acute-SIV infection. The possible mechanisms of Δ9-THC-induced improvement of BDNF expression and decreased neuroinflammation are currently being investigated. Future studies will determine if Δ9-THC-mediated modulation of epigenetic mechanisms provides neuroprotection in other regions of the brain and if Δ9-THC can provide protection during chronic SIV infection.

Supplementary Material

Refer to Web version on PubMed Central for supplementary material.

Acknowledgments

This study was supported by National Institutes of Health grants: R01 DA030053 (NIH/NIDA), P60AA09803 (Analytical Core Laboratory LSUHSC Alcohol Research Center) and OD011104 (formerly RR00164). We acknowledge the scientific and technical expertise of John Maxi, graduate student at LSUHSC-NO, in dissecting the striatum from the brains. The authors would like to thank Drs. Ronald S. Veazey and Andrew A. Lackner for their scientific expertise. The authors also acknowledge Maurice Duplantis, Yun Te Lin, Faith R. Schiro and Cecily C. Midkiff for their technical assistance in the study.

References

Altuvia Y, et al. Clustering and conservation patterns of human microRNAs. Nucleic acids research. 2005; 33:2697–2706.10.1093/nar/gki567 [PubMed: 15891114]

Anderson AM, et al. Plasma and cerebrospinal fluid biomarkers predict cerebral injury in HIV-infected individuals on stable combination antiretroviral therapy. Journal of acquired immune deficiency syndromes. 201510.1097/QAI.0000000000000532

Antinori A, et al. Updated research nosology for HIV-associated neurocognitive disorders. Neurology. 2007; 69:1789–1799.10.1212/01.WNL.0000287431.88658.8b [PubMed: 17914061]

Avraham HK, Jiang S, Lee TH, Prakash O, Avraham S. HIV-1 Tat-mediated effects on focal adhesion assembly and permeability in brain microvascular endothelial cells. J Immunol. 2004; 173:6228–6233. [PubMed: 15528360]

Bachis A, Avdoshina V, Zecca L, Parsadanian M, Mocchetti I. Human immunodeficiency virus type 1 alters brain-derived neurotrophic factor processing in neurons. The Journal of neuroscience : the official journal of the Society for Neuroscience. 2012; 32:9477–9484.10.1523/JNEUROSCI.0865-12.2012 [PubMed: 22787033]

Bachis A, Major EO, Mocchetti I. Brain-derived neurotrophic factor inhibits human immunodeficiency virus-1/gp120-mediated cerebellar granule cell death by preventing gp120 internalization. The

Journal of neuroscience : the official journal of the Society for Neuroscience. 2003; 23:5715–5722. [PubMed: 12843275]

Bashaw GJ, Klein R. Signaling from axon guidance receptors. Cold Spring Harbor perspectives in biology. 2010; 2:a001941.10.1101/cshperspect.a001941 [PubMed: 20452961]

Berrier AL, Yamada KM. Cell-matrix adhesion. Journal of cellular physiology. 2007; 213:565–573.10.1002/jcp.21237 [PubMed: 17680633]

Buckner RL, Andrews-Hanna JR, Schacter DL. The brain's default network: anatomy, function, and relevance to disease. Annals of the New York Academy of Sciences. 2008; 1124:1–38.10.1196/annals.1440.011 [PubMed: 18400922]

Cabral GA, Griffin-Thomas L. Cannabinoids as therapeutic agents for ablating neuroinflammatory disease. Endocrine, metabolic & immune disorders drug targets. 2008; 8:159–172.

Carlino D, et al. Low serum truncated-BDNF isoform correlates with higher cognitive impairment in schizophrenia. Journal of psychiatric research. 2011; 45:273–279.10.1016/j.jpsychires.2010.06.012 [PubMed: 20630543]

Carmona-Saez P, Chagoyen M, Tirado F, Carazo JM, Pascual-Montano A. GENECODIS: a web-based tool for finding significant concurrent annotations in gene lists. Genome biology. 2007; 8:R3.10.1186/gb-2007-8-1-r3 [PubMed: 17204154]

Chan WC, Lin WC. MetaMirClust: Discovery and Exploration of Evolutionarily Conserved miRNA. Clusters Methods in molecular biology. 201510.1007/7651_2015_237

Chandra LC, et al. Chronic administration of Delta9-tetrahydrocannabinol induces intestinal anti-inflammatory microRNA expression during acute simian immunodeficiency virus infection of rhesus macaques. Journal of virology. 2015; 89:1168–1181.10.1128/JVI.01754-14 [PubMed: 25378491]

Chao CC, Ma YL, Lee EH. Brain-derived neurotrophic factor enhances Bcl-xL expression through protein kinase casein kinase 2-activated and nuclear factor kappa B-mediated pathway in rat hippocampus. Brain pathology. 2011; 21:150–162.10.1111/j.1750-3639.2010.00431.x [PubMed: 20731656]

Chao MV, Lee FS. Neurotrophin survival signaling mechanisms. Journal of Alzheimer's disease : JAD. 2004; 6:S7–11. [PubMed: 15665417]

Cho HJ, Hwang YS, Mood K, Ji YJ, Lim J, Morrison DK, Daar IO. EphrinB1 interacts with CNK1 and promotes cell migration through c-Jun N-terminal kinase (JNK) activation. The Journal of biological chemistry. 2014; 289:18556–18568.10.1074/jbc.M114.558809 [PubMed: 24825906]

Choi CH, Hao L, Narayan SP, Auyeung E, Mirkin CA. Mechanism for the endocytosis of spherical nucleic acid nanoparticle conjugates. Proceedings of the National Academy of Sciences of the United States of America. 2013; 110:7625–7630.10.1073/pnas.1305804110 [PubMed: 23613589]

Clark-Langone KM, et al. Biomarker discovery for colon cancer using a 761 gene RT-PCR assay. BMC genomics. 2007; 8:279.10.1186/1471-2164-8-279 [PubMed: 17697383]

Cosker KE, Segal RA. Neuronal signaling through endocytosis. Cold Spring Harbor perspectives in biology. 2014; 610.1101/cshperspect.a020669

Curinga G, Smith GM. Molecular/genetic manipulation of extrinsic axon guidance factors for CNS repair and regeneration. Experimental neurology. 2008; 209:333–342.10.1016/j.expneurol.2007.06.026 [PubMed: 17706643]

Ehrhart J, et al. Stimulation of cannabinoid receptor 2 (CB2) suppresses microglial activation. Journal of neuroinflammation. 2005; 2:29.10.1186/1742-2094-2-29 [PubMed: 16343349]

ElSohly MA, de Wit H, Wachtel SR, Feng S, Murphy TP. Delta9-tetrahydrocannabivarin as a marker for the ingestion of marijuana versus Marinol: results of a clinical study. Journal of analytical toxicology. 2001; 25:565–571. [PubMed: 11599601]

Fiore R, Schratt G. MicroRNAs in synapse development: tiny molecules to remember. Expert opinion on biological therapy. 2007; 7:1823–1831.10.1517/14712598.7.12.1823 [PubMed: 18034648]

Fraga D, Raborn ES, Ferreira GA, Cabral GA. Cannabinoids inhibit migration of microglial-like cells to the HIV protein Tat. Journal of neuroimmune pharmacology : the official journal of the Society on NeuroImmune Pharmacology. 2011; 6:566–577.10.1007/s11481-011-9291-6 [PubMed: 21735070]

Gannon P, Khan MZ, Kolson DL. Current understanding of HIV-associated neurocognitive disorders pathogenesis. Current opinion in neurology. 2011; 24:275–283.10.1097/WCO.0b013e32834695fb [PubMed: 21467932]

Garcia KL, et al. Altered balance of proteolytic isoforms of pro-brain-derived neurotrophic factor in autism. Journal of neuropathology and experimental neurology. 2012; 71:289–297.10.1097/NEN.0b013e31824b27e4 [PubMed: 22437340]

Glass JD, Wesselingh SL, Selnes OA, McArthur JC. Clinical-neuropathologic correlation in HIV-associated dementia. Neurology. 1993; 43:2230–2237. [PubMed: 8232935]

Glazov EA, McWilliam S, Barris WC, Dalrymple BP. Origin, evolution, and biological role of miRNA cluster in DLK-DIO3 genomic region in placental mammals. Molecular biology and evolution. 2008; 25:939–948.10.1093/molbev/msn045 [PubMed: 18281269]

Harezlak J, et al. Persistence of HIV-associated cognitive impairment, inflammation, and neuronal injury in era of highly active antiretroviral treatment. AIDS. 2011; 25:625–633.10.1097/QAD.0b013e3283427da7 [PubMed: 21297425]

Hasler G. Pathophysiology of depression: do we have any solid evidence of interest to clinicians? World psychiatry : official journal of the World Psychiatric Association. 2010; 9:155–161.

Huang da W, Sherman BT, Lempicki RA. Bioinformatics enrichment tools: paths toward the comprehensive functional analysis of large gene lists. Nucleic acids research. 2009a; 37:1–13.10.1093/nar/gkn923 [PubMed: 19033363]

Huang da W, Sherman BT, Lempicki RA. Systematic and integrative analysis of large gene lists using DAVID bioinformatics resources. Nature protocols. 2009b; 4:44–57.10.1038/nprot.2008.211 [PubMed: 19131956]

Hurtrel B, Chakrabarti L, Hurtrel M, Maire MA, Dormont D, Montagnier L. Early SIV encephalopathy. Journal of medical primatology. 1991; 20:159–166. [PubMed: 1942006]

Kent WJ, Sugnet CW, Furey TS, Roskin KM, Pringle TH, Zahler AM, Haussler D. The human genome browser at UCSC. Genome research. 2002; 12:996–1006. Article published online before print in May 2002. 10.1101/gr.229102 [PubMed: 12045153]

Kong D, et al. Inflammation-induced repression of tumor suppressor miR-7 in gastric tumor cells. Oncogene. 2012; 31:3949–3960.10.1038/onc.2011.558 [PubMed: 22139078]

Laddha SV, et al. Genome-wide analysis reveals downregulation of miR-379/miR-656 cluster in human cancers. Biology direct. 2013; 8:10.10.1186/1745-6150-8-10 [PubMed: 23618224]

Lim BK, Matsuda N, Poo MM. Ephrin-B reverse signaling promotes structural and functional synaptic maturation in vivo. Nature neuroscience. 2008; 11:160–169.10.1038/nn2033 [PubMed: 18193042]

Melli G, Keswani SC, Fischer A, Chen W, Hoke A. Spatially distinct and functionally independent mechanisms of axonal degeneration in a model of HIV-associated sensory neuropathy. Brain : a journal of neurology. 2006; 129:1330–1338.10.1093/brain/awl058 [PubMed: 16537566]

Meulendyke KA, et al. Elevated brain monoamine oxidase activity in SIV- and HIV-associated neurological disease. The Journal of infectious diseases. 2014; 210:904–912.10.1093/infdis/jiu194 [PubMed: 24688074]

Mocchetti I, Bachis A. Brain-derived neurotrophic factor activation of TrkB protects neurons from HIV-1/gp120-induced cell death. Critical reviews in neurobiology. 2004; 16:51–57. [PubMed: 15581399]

Molina PE, Amedee A, LeCapitaine NJ, Zabaleta J, Mohan M, Winsauer P, Vande Stouwe C. Cannabinoid neuroimmune modulation of SIV disease. Journal of neuroimmune pharmacology : the official journal of the Society on NeuroImmune Pharmacology. 2011a; 6:516–527.10.1007/s11481-011-9301-8 [PubMed: 21830069]

Molina PE, et al. Modulation of gut-specific mechanisms by chronic delta(9)-tetrahydrocannabinol administration in male rhesus macaques infected with simian immunodeficiency virus: a systems biology analysis. AIDS research and human retroviruses. 2014; 30:567–578.10.1089/AID.2013.0182 [PubMed: 24400995]

Molina PE, et al. Cannabinoid administration attenuates the progression of simian immunodeficiency virus. AIDS research and human retroviruses. 2011b; 27:585–592.10.1089/AID.2010.0218 [PubMed: 20874519]

Mowla SJ, Farhadi HF, Pareek S, Atwal JK, Morris SJ, Seidah NG, Murphy RA. Biosynthesis and post-translational processing of the precursor to brain-derived neurotrophic factor. The Journal of biological chemistry. 2001; 276:12660–12666.10.1074/jbc.M008104200 [PubMed: 11152678]

Nelson AB, Kreitzer AC. Reassessing models of basal ganglia function and dysfunction. Annual review of neuroscience. 2014; 37:117–135.10.1146/annurev-neuro-071013-013916

Nogales-Cadenas R, et al. GeneCodis: interpreting gene lists through enrichment analysis and integration of diverse biological information. Nucleic acids research. 2009; 37:W317–322.10.1093/nar/gkp416 [PubMed: 19465387]

Noorbakhsh F, et al. MicroRNA profiling reveals new aspects of HIV neurodegeneration: caspase-6 regulates astrocyte survival. FASEB journal : official publication of the Federation of American Societies for Experimental Biology. 2010; 24:1799–1812.10.1096/fj.09-147819 [PubMed: 20097875]

Presutti C, Rosati J, Vincenti S, Nasi S. Non coding RNA and brain. BMC neuroscience. 2006; 7(Suppl 1):S5.10.1186/1471-2202-7-S1-S5 [PubMed: 17118159]

Raedler TJ. Inflammatory mechanisms in major depressive disorder. Current opinion in psychiatry. 2011; 24:519–525.10.1097/YCO.0b013e32834b9db6 [PubMed: 21897249]

Ramirez SH, Sanchez JF, Dimitri CA, Gelbard HA, Dewhurst S, Maggirwar SB. Neurotrophins prevent HIV Tat-induced neuronal apoptosis via a nuclear factor-kappaB (NF-kappaB)-dependent mechanism. Journal of neurochemistry. 2001; 78:874–889. [PubMed: 11520908]

SAMSHA. Results from the 2004 National Survey on Druge Use and Health: National Findings. Rockville, MD: 2005. vol NSDUH Series H-36

Sanders VJ, Everall IP, Johnson RW, Masliah E. Fibroblast growth factor modulates HIV coreceptor CXCR4 expression by neural cells. HNRC Group Journal of neuroscience research. 2000; 59:671–679.

Sardar AM, Czudek C, Reynolds GP. Dopamine deficits in the brain: the neurochemical basis of parkinsonian symptoms in AIDS. Neuroreport. 1996; 7:910–912. [PubMed: 8724671]

Smrt RD, et al. MicroRNA miR-137 regulates neuronal maturation by targeting ubiquitin ligase mind bomb-1. Stem Cells. 2010; 28:1060–1070.10.1002/stem.431 [PubMed: 20506192]

Soundararajan P, Fawcett JP, Rafuse VF. Guidance of postural motoneurons requires MAPK/ERK signaling downstream of fibroblast growth factor receptor 1. The Journal of neuroscience : the official journal of the Society for Neuroscience. 2010; 30:6595–6606.10.1523/JNEUROSCI.4932-09.2010 [PubMed: 20463222]

Szulwach KE, et al. Cross talk between microRNA and epigenetic regulation in adult neurogenesis. The Journal of cell biology. 2010; 189:127–141.10.1083/jcb.200908151 [PubMed: 20368621]

Tabas-Madrid D, Nogales-Cadenas R, Pascual-Montano A. GeneCodis3: a non-redundant and modular enrichment analysis tool for functional genomics. Nucleic acids research. 2012; 40:W478–483.10.1093/nar/gks402 [PubMed: 22573175]

Tatro ET, et al. Evidence for Alteration of Gene Regulatory Networks through MicroRNAs of the HIV-infected brain: novel analysis of retrospective cases. PloS one. 2010; 5:e10337.10.1371/journal.pone.0010337 [PubMed: 20436668]

Tracey I, Lane J, Chang I, Navia B, Lackner A, Gonzalez RG. 1H magnetic resonance spectroscopy reveals neuronal injury in a simian immunodeficiency virus macaque model. Journal of acquired immune deficiency syndromes and human retrovirology : official publication of the International Retrovirology Association. 1997; 15:21–27.

Tsuchiya S, Okuno Y, Tsujimoto G. MicroRNA: biogenetic and functional mechanisms and involvements in cell differentiation and cancer. Journal of pharmacological sciences. 2006; 101:267–270. [PubMed: 16921236]

Winkler JM, Chaudhuri AD, Fox HS. Translating the brain transcriptome in neuroAIDS: from non-human primates to humans. Journal of neuroimmune pharmacology : the official journal of the Society on NeuroImmune Pharmacology. 2012; 7:372–379.10.1007/s11481-012-9344-5 [PubMed: 22367717]

Winsauer PJ, et al. Tolerance to chronic delta-9-tetrahydrocannabinol (Delta(9)-THC) in rhesus macaques infected with simian immunodeficiency virus. Experimental and clinical psychopharmacology. 2011; 19:154–172.10.1037/a0023000 [PubMed: 21463073]

Witwer KW, Sarbanes SL, Liu J, Clements JE. A plasma microRNA signature of acute lentiviral infection: biomarkers of central nervous system disease. AIDS. 2011; 25:2057–2067.10.1097/QAD.0b013e32834b95bf [PubMed: 21857495]

Yang X, Gabuzda D. Regulation of human immunodeficiency virus type 1 infectivity by the ERK mitogen-activated protein kinase signaling pathway. Journal of virology. 1999; 73:3460–3466. [PubMed: 10074203]

Yelamanchili SV, Chaudhuri AD, Chen LN, Xiong H, Fox HS. MicroRNA-21 dysregulates the expression of MEF2C in neurons in monkey and human SIV/HIV neurological disease. Cell death & disease. 2010; 1:e77.10.1038/cddis.2010.56 [PubMed: 21170291]

Zhang Y, Zhang R, Su B. Diversity and evolution of MicroRNA gene clusters Science in China Series C. Life sciences/Chinese Academy of Sciences. 2009; 52:261–266.10.1007/s11427-009-0032-5

Zhou L, et al. A parallel genome-wide mRNA and microRNA profiling of the frontal cortex of HIV patients with and without HIV-associated dementia shows the role of axon guidance and downstream pathways in HIV-mediated neurodegeneration. BMC genomics. 2012; 13:677.10.1186/1471-2164-13-677 [PubMed: 23190615]

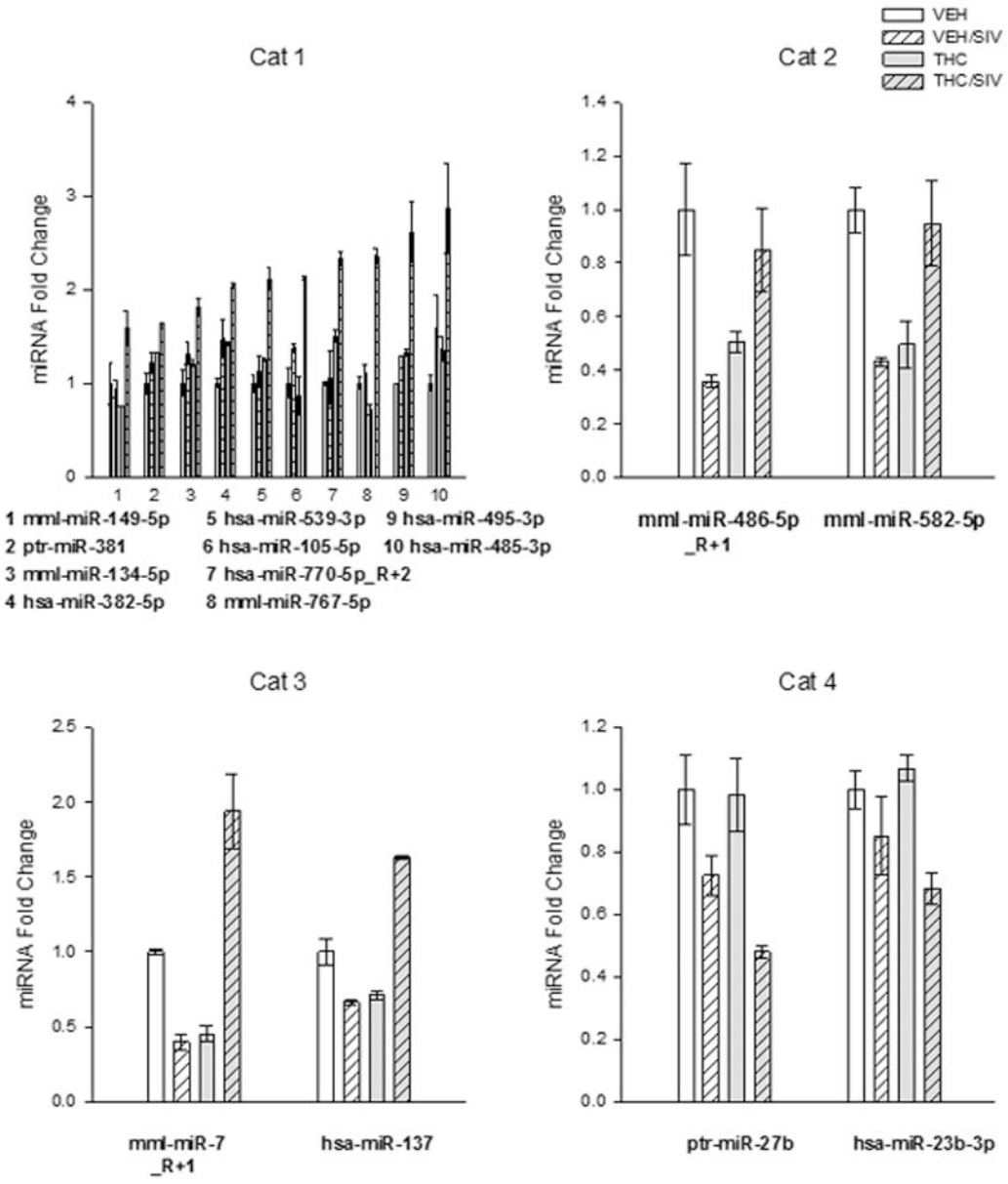

Fig. 1.

Differential expression of miRs in the striatum of macaques during acute-SIV infection and chronic THC administration. Category 1 - miRs that were increased in THC/SIV, but did not differ between VEH/SIV and VEH groups. Category 2 - miRs that were decreased in VEH/SIV and THC animals, but did not differ between VEH and THC/SIV groups. Category 3 - miRs that were increased in the THC/SIV as compared with the VEH group. Category 4- miRs that were decreased in THC/SIV compared with the VEH group. The reads of VEH/SIV, THC/SIV and THC were normalized to the reads of VEH to obtain the fold-change. Values are means±SEM.

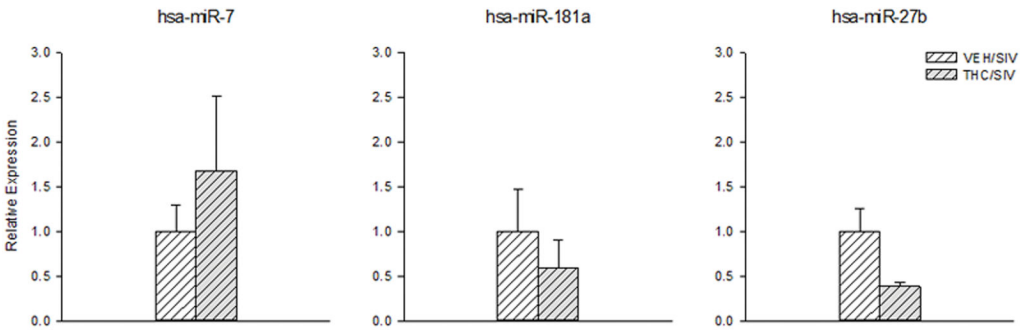

Fig. 2.

Relative miRNA expression of miR-7, miR-181a and miR-27b in the striatum of THC/SIV (hatched bars) and VEH/SIV macaques (hatched shaded bars) determined by qPCR. Values are mean±SEM.

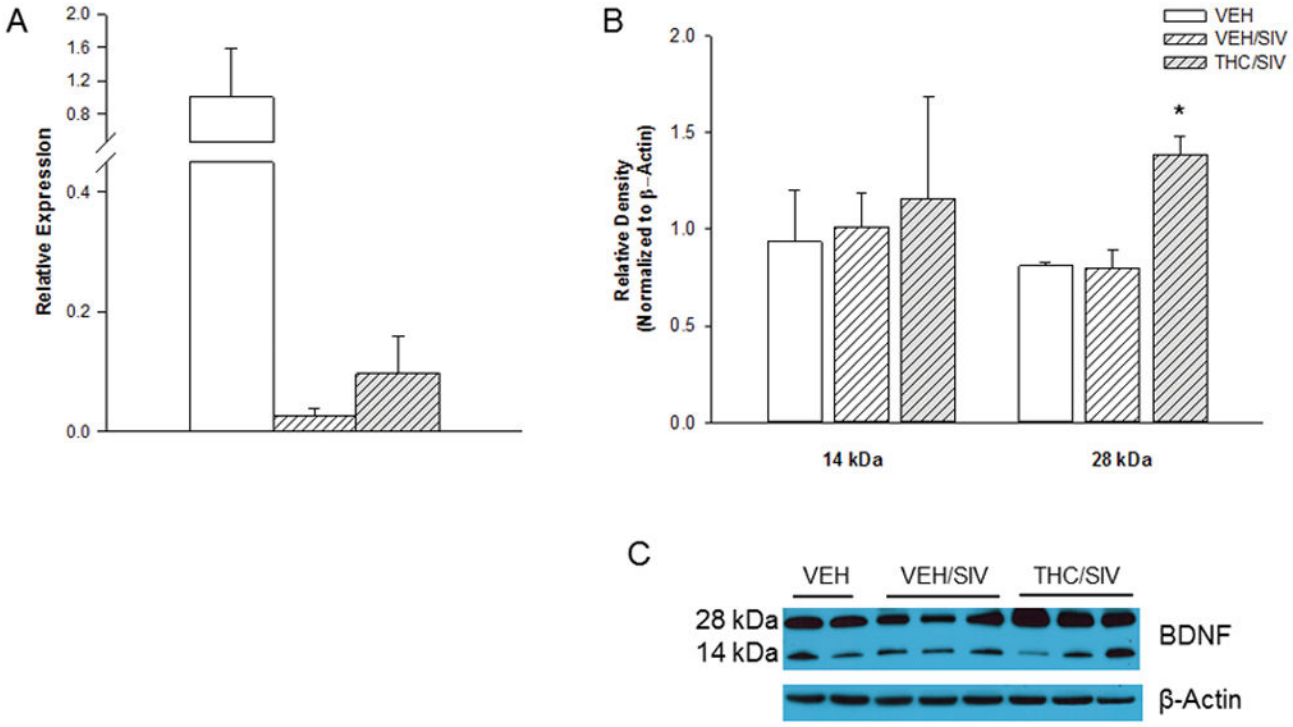

Fig. 3.

Expression of BDNF in the striatum of macaques of VEH (open bars), VEH/SIV (hatched bars), and THC/SIV (hatched and shaded bars) macaques. A) BDNF mRNA expression relative to controls B) BDNF protein expression relative to controls C) Representative western blot image of BDNF levels in the striatum of macaques. Values are means±SEM. *p<0.05 vs. VEH and VEH/SIV.

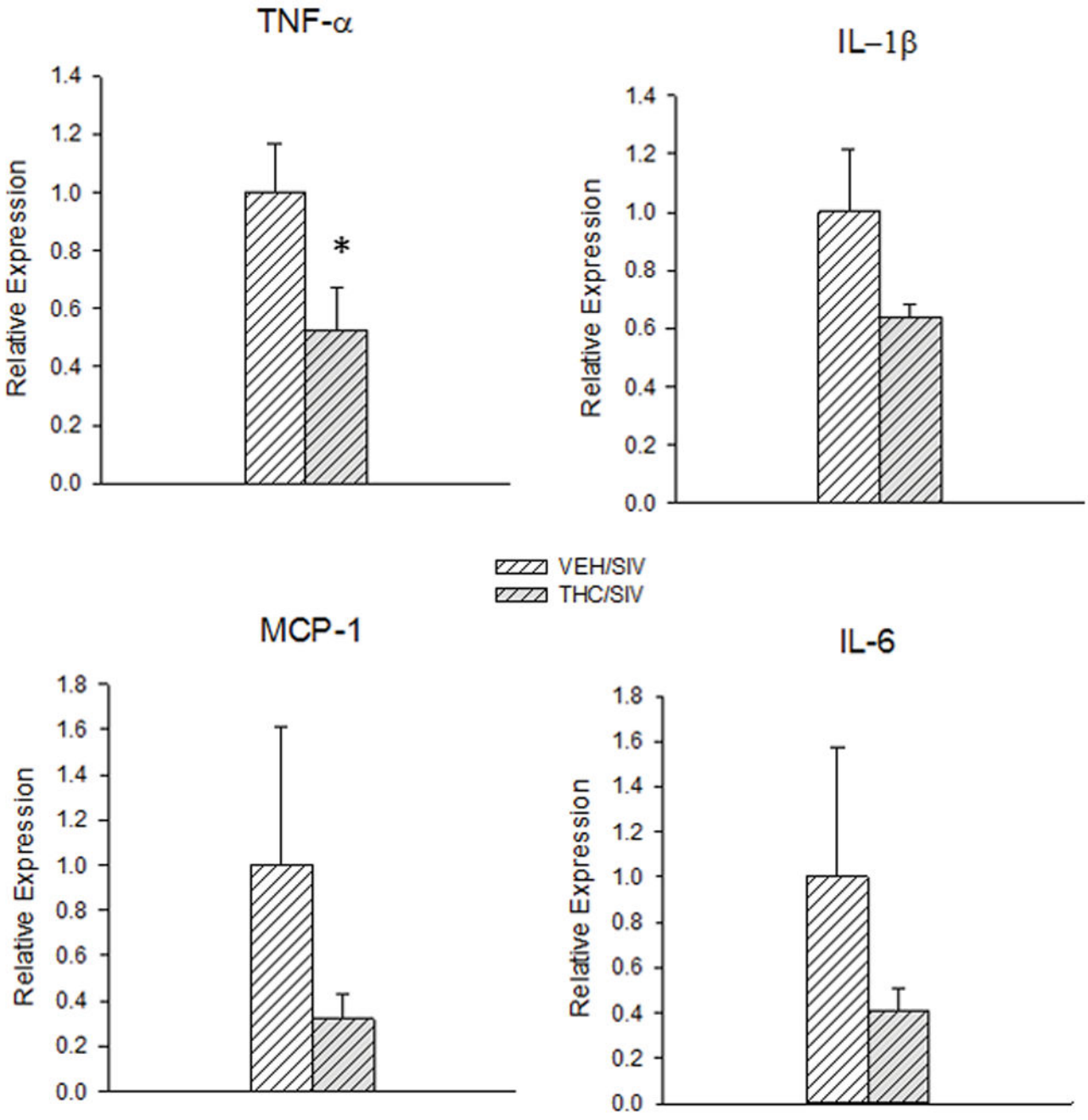

Fig. 4.

Relative mRNA expression of TNF-α, IL-1β, MCP-1, and IL-6 in the striatum of THC/SIV (hatched and shaded bars) and VEH/SIV macaques (hatched bars). Values are mean±SEM, N=4/group. *p<0.05 vs. VEH/SIV.

Table 1

THC-dependent increase in miR expression in the striatum during acute-SIV infection. miR name, predicted or validated target genes are shown.

Category	miR	Target gene
1 – Increased miR expression due to THC in the presence of SIV	hsa-miR-382-5p	TOP1, SLCO1A2, ENKUR, FOXN2, CDK13, DDX3X, STXBP4, MIA3, MEIR5, OLA1, UBTF
	hsa-miR-485-3p	ADAMTSL5, GPI, C14orf184, CYTH, RAB8B, RFT1, EFHC1, CNKSR3, ST3GAL1, SSH3, EPB41L4A, BSG, TNFSF9,FBRS, STMN1, PRIM2, RBM4, TTBK1, TMEM214, TMEM132D, POLE, ZBTB3, PPIE, KIAA1328, MTFMT, WHSC1, SLC26A9, ZNF527, UNC45A, NUCB1, PTMS, NWD1, DUSP16, DCP1A, C8orf80, TAOK1, SDC3, ADIPOR2, PARP11, OPA1, ALG1, TREML2, FCRLA, EGF, ARSA, GPR132, WDR55, ZNF528, ETV7, LXN, PCBD2, FGD2, STX5, NDRG3, PNPLA5, DNAJC5G, TPD52L2, SH3TC2, IGHMBP2, EHMT1, F2RL2, ZC3HAV1L, PLEKHO2, EFCAB2, SKA1, NTM, HHAT, TM4SF20, UTP20, CCR5, PL-5283, RAD18 PLEKHA5, CYP1A2, BMP8A, ZDHHC18, MFI2, SNX20, CYP11B1, CTF1, IBA57, HIF3A, RPRD1B, FAM18A, FSTL3, NTRK3, GLT1D1, TIMM13, WDR35, SLC16A2, HMGA2, TIMM50, CDKAL1, CLCC1, UBE2D4, MEFV, ZBTB39, ATP6 V0D2, SLC36A3, UBA52, TRIM40, ZNF850, MICU1, ZNF346, ZC3H12D, ETNK2, EMILIN3, RASD2, LYG1, KIAA1383, EIF2C4, TMEM53, FTO, PEX12, AFG3L2, CRTAP, ZNF343, ZNF648, DNAJC19, UROC1, SEZ6L, LDLRAD3, ZKSCAN1, GPN3, ETNK1, MDM4, GTF2H3, RWDD4, MEOX1, CRIPT, MRPL35, ZNF814, EARS2, VPS26A, CWF19L1, AFAP1, MPZL2, INPP5A, APOBEC3F C17orf102, ZNF641, TDRKH, ITPRIP, EEF2K, CD200, IL17A PPARGC1A, ZNF155, PLIN3, ABR, CAPN5, VTA1, ZNF81, CKS1B, ALDH16A1, ZNF497, GJB2, ZNF764, RNF24, MGAT5B, TMPRSS4, SPTB, EPB41L2, CD300LG, NXPH3, ZNF578, DES, PHTF2, ALOX15, ACTR3, ZNF474, MAP6D1, SLC29A2, GLB1L3, SGSM2, ANKS4B, GNAL, RMND5B, MRPS27, KCNA6, BAIAP3, ZNF831, OAS1, CYorf15B, ALX4 ACTR8, PPIL2, MGST3, ZNF548, TMBIM6, SLC16A14, CAV2, NNT, WBP2NL, ZNF716, EIF4A1, EIF2AK2, C16orf70, PHC2, IRAK4
	hsa-miR-495-3p	CD9, CLDN10, APOL6, PRKAG2, CADPS2, DDIT4, UNG, OTUD4, PSAPL1, AGBL4, DMRTC2, ST18, TNFRSF1B, ASB5, PLEKHF2, HNF4G, DEPDC5, RAVER2, PPP1R2, PCDHB9, UBE3A, TNC, SLC2A10, FZD4, KDM5D, OR11A1, ELL2, NUP62CL, PBOV1, S1PR3, ELF1, CTNND2, CAST, CT47B1, THBS2, MED12L, POLR3G, AK5, RBM20, HJURP, ZNF599, HSPA13, LYRM7, ATP7A, MAPKBP1, NLN, PRUNE2, CADM1, HESX1, C11orf82, MDC1, DCAF17, BUB1, NLGN1
	hsa-miR-539-3p	LATS1, WBP4, CHORDC1, BTLA, MEGF11, ACSL6, KIAA0232, GPRC5B, RAD50, VPS36, XRN1, DCDC5, METTL15, HS6ST3, CSTA, MFAP5, FNIP1, TBRG1, G2E3, DDHD1, TBK1, PAPD5, CCNYL1, NDFIP1, KLRG1, SPP1, ST8SIA1, NEBL, BTBD7, LCOR, GABRA4, MMP8, RAB5A, HNRNPF, CSRP1, POPDC3, DHTKD1
	miR-153	CLCN5, ANGPT1, HEY2, PMP2, FAM40B, KLF5, FOXR2, DSG2, TBC1D19, KLF13, CHML, UTRN, GIF, PLCB1, LIMS1, YIPF2, SCLT1, PTPN14, ADAM19, RPS6KA5, OSBPL6, SERTAD2, KCNA1, NFE2L2, PPA2, MAP4K5, MOV10, OPRM1, DSE, SLCO5A1, NUFIP1, CELA2A, EYS, PQLC3, NPHP4, HMSD, FABP2, CELA2B, SLC14A1, UNC5C, GALNT7, FXR1, SERAC1, GGCX, TLCD2, NFIA, GFPT2, FBXO8, PHKG2, PTCH1, KDSR, ANK3, ING2, GNPDA2, IDO1, TAF7, NFIB, DDIT4, ME1, USP28, PURA, ANKRD42, FAM110B, SLC25A21, SGCD, MTMR12, CNN3, NEUROD4, CBFB, FBXO4, KCNE1, ISCA2, SLC2A9, WWOX, IL31RA, DPY19L1, SUN2, SPHK2, DMD, GLRA3, RPL22, FAM168B, ZNF443, NEK1, ZNF799, EGFLAM, FEM1C, KCND1, MGAM, RUNDC3B, HNRNPA1, UCKL1, TPCN1, TAGLN3, HTR1F, FAM160A1, NEUROD1, SYT10, PLEKHA3, NPTN, ZCCHC2, TES, RASL12, LDLR, TMED5, PARD6G, POTEC, UBA6, SLC4A4, UBE2W, ASB7, PTPN3, FURIN, PDP2, FRG2, LOC100288255, PCTP, UTY, FZD3, ACTN4, ITSN2, RIC8B, DYRK1A, KCNQ4, NFATC3, FTSJD1, SPATA18, ACTN3, MYNN, ZNF84, KLF3, AUTS2, CIB2, CACNB4, PEA15, TET2, O3FAR1, RASA1, TGFBR2, PGR, NEUROD6, SLC35B4, FAM71F1, COL19A1, ANKRD29, FRG2C, TFEC, MTFR1, ZNF816, ITPR1, TMED10, SLCO4C1, PLEKHG7, SH3BP4, CCDC50, WIPF1, SGK3, C8orf44-SGK3, VWA5B2, ROBO2, TMEM110, MLL, ZNF879, RASSF4, BTBD7, ICAM4, TMEM212, CD109, CREM, GAS8, C7orf58, ENKUR, GATM, NEFL, ZNF41, PARD6B, RYR3, ARF1, ZNFX1, DLG2, B4GALT1, ZCCHC4, ZNF808, ZNF431, EMB, ACTBL2, CD69, DCLRE1B, GRB2, C9orf40, KDM6A
	ptr-miR-381	EGFL6, RAB11FIP2, HOOK3, PENK, LCORL, ZFY, DCUN1D5, TEK, FILIP1L, TES, GPR34, VASH2, PARD6B, USP1, FNIP1, GRM8, PTP4A1, GPR65, ZCCHC11, ZDHHC20, MRS2, ANO4, PCDH8, ARID4B, NUDCD1, APAF1, MAGT1, KIF1B, NOC3L, PPAP2B, ACTBL2, ZFPM2, OAS2, PHYHIPL, CGGBP1, MET, BST1, ATG2B, GRM5, TICAM2, TMED7-TICAM2, CEP76, HCCS, MARK1, SFRP2, ORC4, TMX1, LRP6, KLF3, OTUD6B, HBP1, CWC22, PTCH1, B4GALT6, NETO1, C19orf39, UBR1, NFIA, PNN, C14orf2, TRIM63, BAG1, TMEM14C, WFDC8, TMEM188, ANKS1B,

Category	miR	Target gene
		FAM9C, CHD2, CD46, CD300LG, DHX33, DVL2, ZWILCH, HSPA13, SEMA6D, ZNF521, RAB2A, LGALS8, ATPBD4, MTSS1, KLHL35, ATRN, UBN1, ANKRD50, WIPI1, LRRC4
	hsa-miR-770-5p_R+2	GMFB, ARHGAP12, TRPS1, MYO6, ZCCHC2, SLC12A6, AKIRIN2, MESDC1, TMEM178, CPEB3, GRIA2, RCAN2, BTG1, STC1, STK38L, MAPKAP1, CNR1, GGA3, IPMK, AFF3, TP53INP1, SMARCC1, MAGI3, GTDC1, HS2ST1, FAM120C, SORT1, AGFG1, SMCHD1, MAP3K1, NMT2, ZFAND3, PBX1, RARA, PSD3, RYBP, PLXDC2, NETO1, RNF122
	mml-miR-767-5p	COL4A4, DCC, SLC7A11, TMEM169, TMEM236, COL3A1, ZNF644, CSDE1, LOC221710, TET1, BASP1, PMP22, NFIA, HMCN1, NAP1L5, PI15, CBLL1, RPS6KB1, SCAI, MB21D2, SERTAD2, RIMS1, CACNA2D3, ADAM12, DDX5, DAZAP2, MYCN, KLF2, MBTPS2, MYO1D, NLK, PEG10, PLEKHG3, CXADR,XPO4, SMAD6, LRRC8B, HMGCS1, VHL, TCEAL4, DPYSL5, WDFY1, SLC35F3, SESTD1, LYSMD3, EML6, SEMA3C, FBN2, ATXN1, BACH2, PDXDC1, NRAS, ADAMTS3, GRIA3, FGF4, TTC30B, FAM71C, SLC5A7, AP4E1, MTRNR2L1, EPS15, CYCS, OPCML, SBNO1, KLF6, FOXJ2, CTSK, FGF9, EPB41L4B, SELE, DBT, IFFO2, TTC9, RAI14, SLC36A1, ADAMTS2, MEX3B, USP34, HAPLN3, SDC2, TGIF2, SNX1, GRIP1, TET3, PAPOLG, IFI30, C16orf52, ADRBK1, POLE3, NUAK1, CRISPLD1, PL-5283, IREB2, DOPEY1, ACPL2, TBL1XR1
	hsa-miR-105-5p	FLRT2, TJP1, ZNHIT6, TULP4, CAB39, RAB2A, TM9SF2, C1orf168, ST8SIA3, EPHA4, SEL1L, SUZ12, ARHGEF7, HNRNPK, USP15, SNIP1, TLK1, ATAD2B, CREB5, RERG, AP1S3, SLC12A8, REST, YIPF5, SLC31A1, ICA1L, TFCP2, HP1BP3, SNX4, FAM120A, SLC5A1, PRKAB2, KIAA0907, INA, EIF4A2, LDLRAD3, KRT1, APOOL, MRAP2, BCAT1, PIK3IP1, SLITRK4, SIN3A, TEAD1, RAPGEF2, KIAA0240
	mml-miR-134-5p	RAB27A, ANKRD55, STAT5B, TCF21, BNC2, DPH2, ZMAT5, PHLPP2, PPP1R7, LMLN, GGCX, EXD1, TRIM9, TAB1, HNMT, GRIK2, SSBP2, WWOX, CALCOCO2, CISD3, MRS2, MED13, RAN, FAM168B, MFAP3L, SLC30A4, ARL4D, NDFIP2, BDNF, ANGPTL4, RABEP1, NIPA1, CPS1, B3GNT9, KLHL14, GNAO1, MRFAP1, USP9X, GRPEL2, POLR3H, SLC25A5
	mml-miR-149-5p	STARD3, CACHD1, PHLPP2, N4BP3, RAB43, S1PR2, ADCY1, REPS2, RAB3IL1, ISY1-RAB43, KCNS1, RNF2, MTHFR, SLC9A8, PLEKHA8, KCNJ5, CMTM3, NDST1, SLC19A2, AAK1, EDAR, UBIAD1, CCNI, MAP3K13, SLC4A4, MRPL17, RSBN1L, PHLDB1, RPH3AL, LOC388630, MLH3, BRPF3, EDNRA, ZNF597, COX10, BPTF, MRPL3, TCEB3, CEP95, FBXL16, PEA15, C20orf4, OXNAD1, FASLG, SMC1A, RAP1A, TUFT1, GRIA3, SNCAIP, TNFRSF19, MPDU1, SPINK7, HNRNPA1, GDAP2, TMEM234, CORO2B, PAN2, CRTC2, SHMT2, SLCO3A1, C3orf75, CD5, EXT1, HDDC2, BAIAP2L1, DNAJC18, GPAT2, EXOG, FMO2, PDS5A, LMBR1L, PRDX6, CNIH4, PURB, LOC728392, PRPS2, PIP4K2B, TCTA, CLCF1, SHROOM2, C8orf55, C9orf5, EPHB3, SRPK1, NRP2, DET1, IFFO2, PCDH19, EIF5, TNKS, GAB2, CBX5, CYB5B, MTHFSD, SF1, AP1B1, PSCA, TP63, LCMT1, DMRTA2, FOXO4, CCT3, MTMR3, PLEKHH2, OXSR1, RNF220, DAB2IP, APPL2, TSPAN14, CCDC97, BAI1, ADCYAP1R1, MARCKSL1, IGJ, CERS2, AARS2, PDGFRA, SEMA3G, MANBAL, CNTNAP2, TCEANC2, SLC9A3R1, SGTA, AMOTL2, UBFD1, TRPM7, INTS3, SYT7, FAM18B2, CACNG4, SIRPB2, POLDIP2, OTUB2, ASB4, VTCN1, C7orf63, FBXW4, SSTR1, FZD5, SEMA6C, BBC3

Table 2

SIV-dependent decrease in miR expression that is restored to VEH levels by chronic THC. miR name, validated or predicted target genes are shown.

Category	miR	Target gene
2 – Decreased miR expression due to SIV, and THC restores it to VEH levels	mml-miR-486-5p_R+1	FOXO1, GPX8, PTEN, TRAPPC6B, TWF1, FAM108B1, CCDC85C, PLAGL2, EPB41L1, COL6A6, CELF2, ST5, AFF3, SRSF3, ARID4B, ST6GALNAC6, HAT1, RFFL, GABRB3, SP5, TTC28, CSPG5, ARMC8, ZNRF2, ODZ2, TOB1, ZC3HAV1, DOCK3, GPR153, OLFM4, CTDSPL2, PHIP, PIM1, EPHA3, DCBLD2, SLC4A8, NFE2L1, RASSF3, TRHDE, TANC1, BAHCC1, FGF9, TXLNG, UNC5C, SNRPD1, COPS7B, DCC, NR2C2, FAT3, CLDN10, GRHL2, ZNF740, DNAJC21
	mml-miR-582-5p	FOXO1, GPX8, PTEN, TRAPPC6B, TWF1, FAM108B1, CCDC85C, PLAGL2, EPB41L1, COL6A6, CELF2, ST5, AFF3, SRSF3, ARID4B, ST6GALNAC6, HAT1, RFFL, GABRB3, SP5, TTC28, CSPG5, ARMC8, ZNRF2, ODZ2, TOB1, ZC3HAV1, DOCK3, GPR153, OLFM4, CTDSPL2, PHIP, PIM1, EPHA3, DCBLD2, SLC4A8, NFE2L1, RASSF3, TRHDE, TANC1, BAHCC1, FGF9, TXLNG, UNC5C, SNRPD1, COPS7B, DCC, NR2C2, FAT3, CLDN10, GRHL2, ZNF740, DNAJC21, TAOK1, GIMAP2, MAP3K1, SHCBP1, FLJ36031, TMEM19, PLA2G12A, KCNC2, CREM, TRIM36, IKBKAP, ANKS1A, LAPTM4B, NOV, IMPG2, IL20RA, GCFC1, ABHD10, ITGA2, GLCE, FRMD6, OR4N4, THAP5, KIAA0146, LRIF1, TET3, CLEC2D, AGPHD1, PEX5, RPS29, C4orf22, C8orf83, UBE2H, PCDH11Y, CAPZA2, RALGAPB, RASL11B, PTPRJ, PRKAA1, ZNF627, GLTSCR1, METAP1, ABHD5, FUNDC1, RUNX3, FOXG1, ZNF354A, BMP10, ELAVL3, SST, MAGEC1, GIN1, ATP10D, DSG3, CD1B, NDUFAF4, ARHGAP42, CAND1, GABPB1, CSTL1, SPAG9, FAM91A1, TCF12, AKAP13, MRC1, FAM188A, RFC1, COG3, OVGP1, GRIP1, EIF2AK3, C16orf52, ABCC8, NIF3L1, ZNF655, YTHDF3, ACSL6, PPIH, SGIP1, FZD2, ABHD2, ZFHX4, EMP2, SREK1IP1, ABTB2, NFIB, FAM160B1, SMC4, PLEKHM3, CDYL, KIAA1671, TRIP11, CEP55, TMEM177, NKX3-2, ACE, CYP4V2, PHF13, IL15, ARIH2, SAP30BP, PDE7A, MAP3K7, PLXNA2, MFAP3L, PABPC5, STXBP3, PSIP1, CLEC7A, GOLGB1, CMIP, BNIP2, TLX2, TAF1A, FAN1, ANKRD1, ZNRF2, CTH, APPL2, KRTAP13-1, ZNF781, TTK, MAPRE1, ALG10B, AQP4, RAB9B, NAE1, CAP2, CLDN16, RICTOR, ZDHHC20, HNRNPH3, ZNF236, NOVA1, TNFAIP1, GNAO1, PKP2, ANAPC7, STRN3, CRISP2, RAB11A, SLC35A2, TBL1XR1, CHN2, RBMS3, EXPH5, COL5A2

Table 3

SIV-dependent decrease in miR expression that is increased by chronic THC compared to VEH. miR names, validated or predicted target genes are shown.

Category 3 – Decreased miR expression due to SIV, and THC increases it more than VEH	hsa-miR-137	RAPGEF5, ZNF295, RREB1, SIK1, SLC12A2, SNRK, C21orf91, STK40, NCOA3, MED11, TMLHE, GBP3, ZNF343, SH3TC1, IFIT3, C8orf84, CCDC126, C16orf46, SSR3, SPTLC3, TIGD1, COCH, DTNA, DMRTA1, ERLIN2, MED27, GLIPR1, NOX4, ICA1L, SGK494, STATH, TCTN3, PIGY, ZNF621, TBCE, PROL1, SUSD3, DMRT2, TBC1D19, AP3S1, ACSBG2, TXNDC17, TULP3, BRAF, C17orf58, DFFB, PARP4, TMSB15B, RNLS, C3orf64, TNFAIP6, ZNF789AP, RPS13, AQPEP, KIAA1383, WARS2, ANGPT1, HTN1, HTN3, WNT16, PPAPDC1B, FTHL17, DOCK8, C1QTNF7, PTN, ALPI, PXDNL, AFM, RPL11, PRSS16, RHOBTB1, RECQL, ARHGAP24, MTFR1, SMCP,NAALAD2, AGPAT5, ALDH8A1, REG3A,, ZNF124, HLA-DQA2, PCDHB7, DSG3, ALPPL2, CASP3, SIP1, HSD3B2, CCNL2, PLAC8, TJP2, GDPD1, RAD51B, SCAMP1, MAGEA6, UGT2B10, MAPK10, MSRB3, ESRRG, ESRRA, NXT2, COL19A1, SHROOM2, MITF, RAVER2, FNDC5, USP30, HLTF, C20orf111, ZNF710, SLC43A2, NEUROD4, AHCYL2, MPP1, MBD2, KIAA0907, KIT, CCNG2, SERP1, PRR16, HNRPDL, PRADC1, ZAK, ARHGEF18, INPP5A, KDM4A, GPCPD1, TMEM56, SLC6A8, MBTPS2, CYYR1, CXCL12, SLC35A1, SLC4A7, PARP8, TBC1D1, ABHD6, TAF7L, SGCG, NIPBL, SLC35A4, EFR3A, KIAA1409, PRKAB2, ZCCHC2, IFT20, FAM126B, E2F6, NCK1, PDLIM3, TCF12, GCA, SLC16A6, APLN, NEUROD1, GJC1, SNX25, SLC1A5, C3orf58, DR1, SWT1, RWDD4, BAZ1A, C10orf26, MAP3K14, NCOA2, TTC26, PDCD6, PRDM1, C20orf26, CNTN3, FMNL2, KLF15, ATP10A, PIAS2, NRXN3, ABI3BP, APPL2, MBNL2, VPS37A, NEFH, CDC37L1, DDX3X, RAB9A, CLDN22, PABPC4L, HMGN3, TDRD7, ABHD5, NCKAP5, DMRT3, SLMAP, CEP128, CSE1L, STK3, E2F7, C17orf103, TRIM23, KLHL10, KDELR3, CDK6, CDC42, CTBP1, PTGS2, ZNF804A, YBX1, CSE1L, PXN
	mml-miR-7_R+1	IGF1R, CAPZA1, IDE, VPS26A, SLC25A15, ARF4, PFN2, CNO, ZNF549, MMAA, ZNF425, CLEC4M, FPGT, H2AFV, ABCA13, B3GALTL, AQPEP, FCHO2, ZNF557, COLEC12, GLTPD1, DTYMK, ZSCAN29, MOSPD1, TFF3, DLEU7, TMEM97, POLI, INF2, EGLN3, FIGF, GABRA6, REG3G, LRRC8E, IL17RB, TM7SF4, SYNC, ANKRD36B, PRDM6, LOC100287036, ZNF275, ADAMDEC1, LILRA6, INPP5B, DHRS7B, MMEL1, MAPKAP1, DNAH14, SCARB2, NAPG, NQO1, SERPINB5, ACER3, TSPYL4, TLR4, CCDC64B, LNX2, APOA2, TTLL6, GRIN2C, ZNF329, FSD2, QTRTD1, FAM164C, GREM1, KRT74, SDHC, TREM1, ATG4C, NXF1, FAM71E1, ZNF75A, FAM115C, SPATA2, RAF1, POLE4, ZNF828, IRS2, UBXN2B, FOXN3, ZNF395, CACNG7, ZC3H4, SNCA, FAM168B, GJC1, HDLBP, ARID4A, RNF141, KIF16B, C5orf22, PSME3, PIK3CD, CCDC76, SLC6A9, KLF4, SLC25A15, CUL5, SLIT1, GLI3, CNPPD1, ATG4A, LEMD3, NDUFA4, ADAM11, CKAP4, CTSB, PIGH, EGFR, NXT2, PARP1, WASF3, CNOT8, UBLCP1, C1orf226, SMC1A, CAMKK2, VDAC1, C2orf63, ISY1, ITPKC, PTAR1, PRKCB, EIF4EBP2, GEN1, PLAC4, NF2, IDE, CCNI2, RB1, FLJ45513, NSL1, UBE2D4, WDR47, PKP2, UBQLN4, LRRC59, SH3GLB1, TBC1D12, CTSK, OSBPL3, TRIM58, TMEM168, C6orf64, CNOT6, RELA, FAM131B, AMOT, CISD2, UGT3A1, C10orf57, MESDC2, TMEM43, LRRC16A, ACSL4, PAN2, CXorf40A, CD69, DNAJC15, UMPS, FRMD4B, PRR18, CLEC1A, FBXL7, LECT1, RUSC1, TBC1D2B, KRTAP7-1, NDST3, TMX4, GATA5, ZFYVE20, SLC4A7, CALM3, GRP, NR4A3, TAB2, CDK1, KRTAP5-4, ZMYND12, ACTC1, DET1, EXOSC2, FCGR3A, FCGR3B, RGS21, SMUG1, DISC1, UBR5, FNDC4, HERPUD2, HMGN4, CCDC66, RBMX, DSEL, KIAA1919, LOC100132963, MS4A7, EDAR, SLC16A7, TLCD2, RYK, HLA-DOB, SAV1, BTLA, ERLIN2, DCAF12L2

Table 4

THC-dependent decrease in miR expression in the striatum during acute-SIV infection. miR names, validated or predicted target genes are shown.

Category 4 – Decreased miR expression due to THC in the presence of SIV	hsa-miR-23b-3p	KIAA1467, WBP2, PDE4B, ZIC4, MRC1, AUH, C2orf69, PNRC2, ALG6, INTU, DEPDC1, SYT4, COG3, TOP1, RUFY2, POU4F2, PKP4, SLC6A14, SEMA6D, C3orf52, PDE7A, PPP4R4, RAB8B, CDC40, CRISPLD1, LIN54, RALYL, ZNF287 TMOD2, TMED5, FUT9, TMPO, MYCT1, CXCL12, DOCK3, RAB39B, NAP1L5, TMEM33, CTCF, MYH4, SATB1, C13orf34, TXLNG, AB39, TNRC6A, SETD8, NEK6, PRKRIR, SEC14L1, RAD51AP1, CNTLN, NUP50, RBM25, ATP6V1E1, HNF4G, TRAPPC6B, GLB1L3, KLF3, UBL3, ZNF395, APAF1, DPY19L4, PPARGC1A, USP53, QSER1, FBXO32, EXOC3L4, ACSS3, VCAN, COL4A4, THUMPD3, ZNF420, SEC23IP, C1orf96, ITGAL, CDC23, NACC2, EFHA2, SNX5, AMBRA1, TBC1D12, TLK1, SLC12A1, HEXIM1, CNOT6L, LPHN2, AUTS2, MTF1, SLC38A1, ZBTB34, PNMA2, ARHGAP20, TNFAIP3, ALDH1A2, TPST1, PIGX, ANKHD1, NLGN4X, CHUK, UBE2R2, ZDBF2, FGD4, MAP7, FAS, IGSF8, TJP1, UTP23, MAGEA5, MAGEA10-MAGEA5, LRAT, CLDN12, SEC24A, FILIP1, PRDM10, KPNA4, HDX, SREK1IP1, PLCXD3, FKBP5, NLGN4Y, MPP2, SLC1A1, ADCY1, SSH2, MYH1, PIP4K2B, IPMK, STAG3L4, BRWD1, SLC25A36, GHITM, LOC100132963, STK4, CCDC82, TXNRD1, TNFAIP6, POU2F1, BTAF1, FAM126B, LYPLA1, PKNOX1, TCF24, FOXP2, CEP350, BNIP2, IYD
	ptr-miR-27b	RGPD5, RGPD4, RGPD8, RGPD6, HDHD2, ARSJ, APOOL, SNRNP27, ZNF100, SLU7, CNTLN, C9orf6, DCHS2, WDR35, NECAB1, SUSD5, TTC39B, MCM9, TMEM184A, GALNT5, ZNF350, CLEC1A, C15orf29, CDR2, DDX58, ZIC5, ZNF84, ANKRD36B, MOSC1, C9orf80, DYNC2LI1, FOXA3, ZNF470, GLYATL1, FAM150A, COG7, NHEDC1, HSPA1L, MS4A7, INPP4A, MXI1, CCDC85A, SSTR1, CCDC72, CEP57L1, PPM1B, C2orf44, PF4V1, ZDHHC17, KCTD14, GTF2H2, CIAO1, GTF2H2C, GTF2H2D, ZNF124, RTKN2, SLFN5, PSMA1, PSPC1, YPEL1, MYSM1, CMKLR1, ALCAM, D4S234E, ALG10, ABCB5, URB1, ZNF619, ZNF187, TRIM50, ASB11, C15orf43, FBXO45, PF4, STBD1, TCHH, CAB39L, RAD9B, C2orf55, FAS, TMEM126B, ZNF81, LIPT2, DCUN1D4, PLK2, FBXW7, GAB1, NRK, RUNX1, TAB3, GRIA4, SLC24A4, TXLNG, GPAM, ACVR1C, SLC6A1, CDS1, NCOA7, SEMA7A, GRB2, SSH1, TSC1, SLC25A25, ABL2, CKAP4, C10orf137, FGD6, FAM193B, SFRP1, SLC7A11, APPBP2, GCC2, ST6GALNAC3, RALGAPA2, PLEKHH1, CEP135, ARFGEF1, SYNRG, HOXB8, SLC39A11, SMAD9, C1orf173, SPTLC2, PDS5B, AFF4, IGLON5, PALM2, KIAA1109, HOXA5, GXYLT1, B4GALT3, EYA4, KIAA1737, KITLG, RCAN2, PRKX, GORASP1, TNRC18, CSRP2, KCNK2, FAM133B, MAP2K4, MYT1, STAB2, ADORA2B, PSEN1, SNAP25, USP42, SEC22A, ITSN2, OBFC2A, EPB41L4A, CCDC149, TMBIM6, C7orf41, EYA1, PAX9, PPARG, C1orf9, CCNG1, MMD, ALG9, CCNK, ARHGEF26, LPAR6, HOXA13, WISP1, KCNA4, SBF2, ZNF800, SFXN2, KCTD8, ATP6V1A, ZHX1, RELN, PRKCB, TMEM194B, AQP11, SLC9A4, GABRP, ANKRD40, SLITRK1, MBTD1, PLCL2, ZNF329, PDK4, GCA, VPS37A, AKIRIN1, GOLM1, TMUB1, LIN28B, C20orf177, CTH, TXN2, STYK1, VIP, TPR, RPS6KA5, GATC, NOTCH1, ST14, MMP13, ADORA2B, CYP1B1, TRAPPC2P1, EDNRA, EYA4, WEE1, VDR, CYP3A4, PAX3, CCNT1, KHSRP, PAX7

Table 5

Biological processes enriched by target genes of miRs in each category

Category	Biological process of target genes	No. of target genes
1 – Increased miR expression due to THC in the presence of SIV	Regulation of transcription (DNA-dependent-88, RNA polymerase II promoter -43)	135
	Signal transduction	61
	Multicellular organismal development	53
	Cell proliferation (positive regulation -26, negative regulation- 23)	49
	Receptor signaling pathway(Insulin -12, TGF-8, EGF-6, Glutamate-4, ERK-4, Wnt-3, Toll like-3, I-kappa B -3)	43
	Ion transport	39
	Cell differentiation	35
	Protein phosphorylation	33
	Cell adhesion	32
	Synaptic transmission	27
	Protein transport	27
	Interspecies interaction between organisms	23
	Brain development	20
	Negative regulation of apoptotic process	18
	Endocytosis	15
	GTP catabolic process	15
	Response to stress	14
	Ubiquitin-dependent protein catabolic process	13
	Muscle organ development	11
	Glucose homeostasis	9
	Nucleobase-containing compound metabolic process	8
	Cellular respiration	5
	RNA splicing	4
	Viral reproduction	4
	Neuron recognition	4
	Axon guidance	3
	DNA repair	3
	Organ morphogenesis	3
	Positive regulation of angiogenesis	6
	Positive regulation of gene expression	3
	Protein complex assembly	3
	Response to drug	3
	Translation	3

Category	Biological process of target genes	No. of target genes
	Innate immune response	3
	Response to ethanol	3
2 – Decreased miR expression due to SIV, and THC restores it to VEH levels	Regulation of transcription, DNA-dependent	33
	Nuclear mRNA splicing, via spliceosome	33
	Regulation of cell migration	19
	FGF receptor signaling pathway	19
	Axon guidance	12
	Cell adhesion	9
	Signal transduction	5
	Transport	8
	Regulation of mitotic cell cycle	3
	Induction of apoptosis	3
3 – Decreased miR expression due to SIV, and THC increases it more than VEH	Regulation of transcription, DNA-dependent	38
	Signal transduction	27
	Receptor signaling pathway (Toll-like - 10, NGF-4, AR-4, MAPK -3, positive regulation of NF-kappaB-3)	24
	Multicellular organismal development	24
	Transport	20
	Apoptotic process	19
	Immune response	11
	Cell division	8
	Developmental growth	4
	Protein phosphorylation	4
	Axon guidance	4
	Cell fate commitment	4
4 – Decreased miR expression due to THC in the presence of SIV	Regulation of transcription, DNA-dependent	38
	Signal transduction	25
	Transmembrane transport	19
	Cell adhesion	15
	Negative regulation of cell proliferation	13
	Protein phosphorylation	13
	Protein stabilization	12
	Chromatin modification	10
	Apoptotic process	8
	Insulin receptor signaling pathway	7
	Embryo development	7
	Toll signaling pathway	6
	Positive regulation of NF-kappaB cascade	4

Category	Biological process of target genes	No. of target genes
	Embryo development	3
	Innate immune response	3
	Regulation of actin polymerization or depolymerization	3
	Response to toxin	3
	Synapse organization	3
	Response to LPS (3), glucocorticoid (3)	6
	B cell differentiation	6
	Cell morphois	4
	Positive regulation of smooth muscle cell migration	4
	Protein stabilization	3
	Cell growth	3

Table 6

THC-dependent decrease or increase in miR expression in the striatum during acute-SIV infection. miR names, validated or predicted target genes are shown.

	miRs	Target genes
Decreased miR expression due to THC/SIV compared to VEH/SIV	mml-miR-338-5p _R-1	PHC3, SCN9A, HEMGN, KLF2, CUL2, KIAA1370, ESRRG, GOLT1B, GYPA, INTU, TSHZ1, USP25, PCDH20, MSTN, GTPBP10, SMAD5, HESX1, RORA, DLGAP1, GUCY1A3, RAB28, DDX59, RABGGTB, DSC3, TRAT1, COPS2, CDH12, ATP6V0A4, GRINL1A, GCOM1, ADM, DCLRE1B, UBA5, UFM1, KRTAP4-8, PABPC4L, WDR72, C1orf96, TNPO1, KRTAP4-11, ETS1, AIMP1, STAU2, IL6, GALNT7, C14orf28, FIGNL2, LIN28B, TRIM71, IGDCC3, ARID3B, STARD9, PTAFR, THRSP, PRR23A, SMARCAD1, YOD1, FIGN, TTLL4, PRTG, C9orf40, C18orf21, SERF2, KCTD21, PXT1, ARHGEF38, DNA2, ZBP1, TGFBR1, RPL36A, SLC5A9, CYP4F2, BRWD1, GDF6, COIL, SIGLEC14, XKR8, LRIG3, NPHP3, MRS2, ZCCHC9, SYNC, SLC35D2, ACVR1C, LRIG2, BZW1, GNPTAB, NDUFA4, CDC34, ZNF322A, THAP9, HIF1AN, ADRB2, DDX19B, DDX19A, ESR2, GALNT1, DDI2, SMC1A, MAP4K3, ERCC6, ABT1, PGRMC1, PARS2, DTX2, MED28, HIC2, ZNF583, KCNJ11, ARG2, PPP1R15B, GATM, CCNJ, KIAA1429, DDTL, CPEB1,HAND1, KHNYN, ATPAF1, LIPT2, BRF2, IGF1R, RPUSD3, DCLRE1B, ZNF215, ZNF341, CNTRL, FMO4, GPCPD1, C8orf58, GJC1, POLR2D, MED8, FAM103A1, OPA3, SFMBT1, FRAS1, CDC25A, RNF170, DVL3, UHRF2, NAP1L1, ZNF347, MYO1H, STX3, APBB3, COL1A2, TMEM2, PPAPDC1B, LHCGR, IGF2BP2, ADAMTS8, SPRYD7, ATG10, DPH3, STARD13, CASP3, SEMA4F, SERPINB9, CLCN5, PLCB2, IGF2BP1, CCNF, SRD5A3, ZNF587, DOK3, ZNF792, TGFBR3, MAP3K1, FNDC3A, ZNF10, ZNF763, CCL7, POM121L12, ACSL6, SIGLEC5, ZFYVE26, ZNF197, LIMD2, SNX6, MAPK6, C5orf62, AHCTF1, HDX, ADAMTS15, KIAA1274, IGSF1, CD200R1, CCDC76, POLQ, STAG3, IL22RA1, PUS7L, RANBP2, TSEN34, ZNF200, MSR1, MARS2, ZNF343, QARS, CD59, TXNDC6, TMEM234, COL3A1, AMACR, GEMIN7, GXYLT1, CPA4, OLFM4, USP12, PLEKHG6, CCR7, SUB1, RBM19, TMEM144, FNDC9, SCN11A, PLA2G2F, BEGAIN, TBKBP1, UFM1, ZNF417, FAM20A, TTC31, ZNF202, RRM2, SDR42E1, TNFSF9, PLXND1, KLHDC8B, HIF3A, LSM11, PLA2G3, UTRN, SSX5, RMI2, SMUG1, DPP3, BTN2A1, ARHGAP28, NEK3, CTPS2, SSX4, CDK6, CDC25A, MYC, BCL2, NKIRAS2, ITGB3, NF2, NRAS, KRAS, PRDM1, LIN41, TRIM71, FOXA1, NR1I2, VDR, RAVER2, HMGA2, HMGA1, EIF2C4, APP, E2F1, WECH, UHRF2, DICER1, HRAS, IGF2, LIN28A, NFKB1, ZFP36L1
	mml-let-7a-5p	
	hsa-miR-151b_R+3	WNT1, SEZ6L, NTRK2, N4BP1, PHF15, CASZ1, WIPI2, SOX12, RIMBP2, SLC12A5, BDNF, NLK, GATA6, CDX2, PLAG1, HOXA11, BCL2, PROX1, KAT2B, CDKN1B, ZNF763, DDIT4, ATM, HIPK2, BCL2L11, HRAS, RNF2, RALA, SIRT1, PRAP1, DUSP6, PTPN11, DUSP5, PTPN22, FOS, MTMR3, KLF6, MCL1, XIAP, GPR78,
	hsa-miR-181a-2-3p	ZNF781, ZNF439, ZNF594, ZNF780B, OSBPL3, PRTG, ZNF780A, RAB3IP, KIAA0528, TMEM87B, PPIP5K2, ATM, NUDT12, FIGN, IL2, FBXO34, TGFBRAP1, TRDMT1, TRIM2, TMEM131, KIAA0195, PDE5A, HOXC8, ZNF83, ZFP36L2, ZFP14, MPP5, SPP1, ACAP2, MARK1, TOM1L1, TXNDC15, CLVS1, MBTPS2, C2orf69, BRAP, SIPA1L2, ZNF563, TMF1, IPO8, S1PR1, ZNF568, FLT1, BTBD3, ARHGEF3, TCERG1, ZNF468, RLF, ITSN1, KLF6, ZNF136, MLL, CTDSPL, SLC4A10, SLC25A37, DDX3Y, MAGOHB, YLPM1, UBP1, RPS6KB1, YTHDC2, C15orf29, PGAP1, ZNF673, METAP1, SYNPR, PITPNB, AFG3L2, FGD4, PBMUCL1, CDON, LPCAT2, DDX3X, HOXD1, ESM1, ZFP62, CLMN, TMEM165, MPP7, PAPD5, ZFP82, PI4K2B, CLIP1, NEK7, ZNF655, KIAA1239, SLC7A2, ACVR2B, ST8SIA4, ZFP36L1, KRAS, PLDN, RALGAPB, PROX1, GPD2, TBC1D1, TIMP3, BRWD1, BIRC6, HSP90B1, CBX7, CLASP1, ETV6, E2F5, APOO, MED8, PAM, GPBP1, PDCD6IP, HEY2, KIAA0182, DNAJC13, CPNE2, CHMP1B, ABI3BP, SPRY4, FHDC1, ATP2B1, LYRM1, GPD1L, BEND3, NLN, CAPRIN1, MKLN1, NR6A1, PHACTR4, BHLHE40, C6orf35, HMBS, TNFRSF11B, TRAK1
	hsa-miR-51b-R+2	
	mml-miR-584-5p_R-1	GBP5, DSG3, ZNF583, MORC3, CCDC152, MCPH1, WWP1, ZNF518A, PPFIA1, MIS12, ACYP2, NEGR1, TTC22, HBS1L, GANAB, POGLUT1, ALPK1, NCOR1, CHORDC1, UHRF1BP1, MAP2, CTXN2, NUFIP2, HDAC1, SETD5, USP6NL, NPHP1, LTBP2, ATP6V1E2, PRRX1, AVPR1A, HSD11B1, SETD1B, MYO5B, ANKRD18A, C3orf23, GC, SEC24D, ZNF765, PDHA1, CYP2J2, AIDA, BTNL3, ZNF585A, MTRF1, PPP2CA, ZNF677, ARL13B, CADPS, LRRIQ3, EIF2AK1, DGKB, FOXN3, NRXN1, CD200, ZNF627, CTDSPL2, ANKLE1, CCDC50, PELI2, FREM1, ANXA1, NAA30, LRRTM3, ANGPTL5, LYPD1 NBN, GTF2A2, SLITRK6, PI15, HBD, H2AFJ, PPM1A, UBTD2, CENPQ, SLC25A40, SIGLEC10, C12orf65, CLSPN, HOOK1, UTP11L, GNG12, VPS41, TWISTNB, CD38, XPO7, UBE4B, AKNAD1, ZNF84, C17orf62, ZNF750, PHF6, C17orf100, ADAMDEC1, C18orf63, THBD, N4BP2L1, SLC35D3, TBRG1, TMX1, PRKCQ, PDIA3, TUSC2, CALB1, SLAMF7, PEX5L, DAND5, ZNF354C, SPOPL, ZNF24, TAZ, C17orf75, LRP11, PTTG1IP
	mml-miR-211	KCNMA1,CDH5, POU3F2, CREB5, ELOVL6, TCF12, RAB22A, IL11, SLC37A3, TMEM237, PHOX2B, FBXO22, AP1S2, PERP, RAB22A, HGSNAT, GSTM3, B3GNT5, TMEM64, FAM126A, TLR6, HAPLN1, SOX14, ZSWIM3, SPOP, ACSM2A, ATP10B, XKR9, EPHA5, BIRC2, MTMR7, THPO, ZCCHC10, ACBD7, C9orf72, USP14, PRAMEF8, POLH, SAMD5,

	miRs	Target genes
		SEMA6A, NTRK2, RASL10A, ACSM2B, AQP11, JRKL, CNOT1, C2orf68, INTS2, PPM1K, BTBD1, LYRM2, EPHB6, FUT10, SOX4, ANGPT1, MYCT1, PRAMEF18, PRAMEF19, TCF12, STYK1, YPEL4, TMEM181, C11orf45, SOS1, TMEM213, ADCY1, RNF170, MAPRE2, ARHGEF33, RHOBTB3, RUNX2, FNDC9, SIX1, MGAT3, IL11, EVC2, ELMO1, GSPT1, ZNF654, VN1R1, PRAMEF12, KIAA0564, DUSP16, CLMP, PTP4A1, MRPS17, ADORA2A, DCUN1D3, SH3PXD2A, KIAA0776, RSPO4, CACNG2, C21orf33, IGFBP5, GTF3C1, CSF2RB, DNAJC13, ZNF629, EPHB2, DUSP19, RAB40B, RAB10, TRIM66, ARHGAP30, WWC3, GPR6, NDRG3, COX5A, POLA1, SLC25A24, C10orf11, C11orf57, TMEM194B, FAM155B, FAM160A2, ACSL4, PIGM, TMEM236, GAL3ST3, UBE2J1, NAPG, SLC43A1, C19orf50, ZC3HAV1, NBR1, SLITRK4, SSRP1, TMEM156, STARD13, TTYH1, SPRYD7, REEP1, MCOLN1, KLLN, MYH15, NOVA1, MAPK9, LOC100507421, CBFA2T3, RGS20, HAS2, RNLS, PDCD6, FRAS1, PLD6, PAM, USP28, DRAP1, PRRX1, GUCA1B, ELAVL2, PTPRD, LRP6, RIMS2, PPIC, FOXC1, EMR3, JPH3, AEBP2, EFNB3, CHP, CAMK1, SLA2, LOC221710, C13orf34, CMBL, SPCS3, SF3B1, SLC4A1AP, DGKG, MMP16, NAA38, ESRRG, ZNF793, TPPP, CCDC144A, RAB13, DHX38, ALPL, DUSP3, PPARGC1A, C1orf43, ACAT1, ERC2, DECR1, PJA1, ZNF423, IL7R, AK4, ALS2, EYS, PLXNA2, C19orf42, NRBF2, C17orf64, NXPH4, MLLT3, PID1, FRS2, FAM168B, EEF1E1, LATS1, CCDC40, ENTHD1, RREB1, SLC12A6, RIOK1, RNF217,
	mml-miR-15b-5p	FGF2, SLC11A2, PLAG1, ZBTB34, MGAT4A, PLSCR4, ANO3, UNC80, TSEN2, TNFSF13B, UBE2Q1, FAM59A, CD80, PISD, CCNE1, TRANK1, SLC13A3, IPO7, CYBASC3, KIAA1432, LOC100130451, FASN, CPEB2, ARL2, PPAPDC2, MTMR3, FCRL2, LAMP3, DCLK1, DNAJB4, PHF19, LY9, GFAP, BCAP29, RUNDC3B, KLHDC8B, MYB, PPPDE2, RPS6KA6, GALNT13, N4BP1, RBM12, RAB9B, PAPPA, GPR63, ERCC6, RASGEF1B, PDK3, USP15, HTR2A, PTPN3, EDA, KIF5A, HAUS3, COL12A1, C2orf42, ZNRF2, UBN2, PAFAH1B2, ACTR2, CBX2, ZFYVE20, PCMT1, FZD10, WEE1, SLC9A8, RS1, ZNF323, MAMSTR, KIF1B, BTBD9, HPSE2, ACVR2B, RAB3B, RNF41, KDSR, SMURF1, UBE4B, STK33, ST8SIA3, ASH1L, YRDC, ZMYM2, GABARAPL1, CDCA4, CD28, CBX4, LSM11, ZC3H13, WNT3A, ODZ2, PHKA1, VPS33B, HELZ, SLC20A2, CNTN3, KIF23, PCGF5, ATXN7L1, EIF4G2, BRWD1, KIF21A, TMC7, ZNHIT6, GNAT1, CCDC19, TNRC6B, LRP6, HTR4, SRPRB, FAM73A, BTAF1, OOEP, SYT10, RSBN1, HSPA1B, PTH, CCDC83, SMAD7, AKT3, USP9X, INSR, FAM91A1, AQP11, DRD1, SIRT4, SNRPB2, PEX13, CDC42SE2, LOC221710, GOLGA1, NELF, CD47, FAM123B, SLC9A6, TMEM100, ATXN7L2, WNK3, MKNK1, MYO5B, KIF5C, CD2AP, C1QL3, RBM6, SRGAP2, C8orf86, SLC12A2, CC2D1B, MAFK, TRPC1, EXT2, ANKRD34C, SLC41A2, PTCD3, WWC1, C10orf46, TMEM55A, ZBTB46, DEPDC5, DZIP1, KCNK10, RSPO3, RAD50, CWC15, ZNF317, IFT74, SHOC2, SYDE2, DMTF1, KIAA1530, UBR3, PRDM4, USP25, NAPG, FGF7, PEX12, C14orf37, GPATCH8, ATXN2, SEL1L3, KIAA0317, ATG14, AXIN2, VEGFA, RBMS1, CHEK1, KCNJ11, TMEM85, NHLRC2, UBE4A, C8orf4, ZNF622, OMG, ATP4B, BTRC, MOBKL3, HSPE1-MOBKL3, GLRX, PAG1, CXorf40B
	mml-miR-500a-3p	TRA2B, RFESD, SLC35A3, PEX2, SNX13, SERBP1, RDH11, SUB1, ABCG5, LEKR1, C12orf77, SATB2, ZBTB41, SIK3, LEPROTL1, GSPT1, CLDN1, PRDM4, PPP2R2A, CBLN4, AHR, PPCS, METTL21A, FGF23, EXOC4, SHISA2, NFE2L2, GATAD2B, DNAJC6, USP28, SH2D1A, LAMA3, CCDC17, NLRP11, IMPAD1, IPO9, TMBIM4, VASH2, UBE3A, ARHGAP20, ZNF274, CCNC, LOC730159, TXNRD1, LRP1B, SMC4, DCLRE1A, PCOLCE2, EFHA2, CROT, TEKT3, FAM116A, C9orf91, TM9SF1, FAM45A, SRSF10, SRSF3, ZFR, EPB41L5, FCHO2, SRGN, TNC, ZNF718, C9orf40, MTMR6, FAM178A, PTPN21, ZNF451, ZNF175, LA2G12A, CLIC4, DACH1, MAPKAPK3, SULF1, LPAR1, ZBTB34, FAM176A, IFRD2, TRABD, IL18BP, TMEM47, CLMN, UBE2L3, IKZF2, GRAMD1C, TRMT2B, HMGCS1, BCL2L15, SKA3, ADI1, ZBTB20
Increased miR expression due to THC/SIV compared to VEH/SIV	mml-miR-7_R+1	
	hsa-miR-137	
	hsa-miR-488-5p_R+2	AR, CYP2E1
	mml-miR-628-5p	LMLN, FAM105A, ATG4A,, RABGEF1, PTN, PLCE1, GOLT1B, KATNAL2, NR1D2, ANK3, ZNF148, DDX59, STK40, ZSCAN22, EFR3A, RAG1, ASCC3, PRTG, SIP1, GRIP1, DMC1, COG6, FAM168B, TXNDC16, BRD9, AP4E1, C3orf19, CISD1, L2HGDH, STX7, UBXN2B, ZNF323, ZNF828, CD80, SMYD1, PIGH, ATXN3, LOC100507203, NXT2, RNF14, KTN1, EMILIN3, PPP1R3D, A1CF, STK24, KIAA0319, DDO, ANP32E, LAPTM4B, CCDC146, CANT1, PTP4A1, BNIP3L, BRMS1L, NBEA, TAF7, ALS2CR11, FUT8, PSTPIP2, PVRIG, EMR2, PLEKHN1, C20orf108, BIRC6, LARS2, ZNF434, HYDIN, RFX4, EAF1, EFCAB4B, SLAMF7, C6orf168, TCEB1, SCN1A, WDR64, BCL6, NSUN7, INSIG1, ZNF793, KCNK2, ERMAP, CCDC144NL, ATP2A2, DOK2, IGFBP3, MGEA5, C1orf141, ZNF791, CAST, SLC26A4, FUT9, RSPH3, XIRP1, OSMR, ERVV-2, BRP44, FNDC5, SLC5A1, MFAP3, ERVV-1, IPO5, TYROBP, SKA1, PDLIM1, BBS1, RASSF8, HTRA1, KREMEN2, ZSWIM1, SLC46A3, COL19A1, LOXL3, NAT2, YAF2, PTGS2, MTDH, GYPA, HNMT, MUC21, PID1, RNF41, ZFP3, NPEPPS, SLC44A5,

	miRs	Target genes
		DCX, SMARCAD1, ST6GAL1, TCF21, AHCYL2, SELS, MAGEA3, MAGEA6, ELOVL1, GPR88, PRR23B, E2F3, SOCS6, KAZN, AHR, RNF169, EIF5A2, ZNF705D, C5orf44, BBS4, CCR1, ARHGAP36, CXCL14, NFE2L3, MLANA, TGM4, NHEJ1, ESRP1, LYPLA1, CGN, COX15, COL4A1, LSM14A, TMEM33, MRPL49, MCU, SPRED1, EPHA3, ALG6, PLD5, SCN3A, HTATIP2, MS4A15, THAP3, SCN2A, PPFIBP1, MYL6, LAMC3, ZCCHC14, NT5E, SLAIN1, ERI1, SETD8, RDH12, LYN, TSPYL1, FKBP5, ZMAT4, ZPLD1, PRKCE, AGTRAP, THRB, GPATCH4, MAGEB3, KLHL9, EPOR, ARF6, ZNF69, ZCCHC24, AARS, KIAA1804, SGMS1, FLRT3, ABRA, C1orf86, BMS1, ZNF207
	mml-miR-299-3p	CUX1, PAIP2B, TCF4, GCFC1, ABCE1, SP4, PRSS22, ADD1, ANK1, KNDC1, CHST2, LUC7L3, MOGS, VEGFA, ENY2, RAB6A, ARAP3, DNAJA2, TMEM155, UBE2H, POGK, ZNFX1
	hsa-miR-105-5p	
	hsa-miR-488-3p	ZNF563, FBN1, C6orf162, FRYL, C7orf41, IGF1, OLFML1, RNGTT, GRIA3, ENAM, PPFIA1, POLR1D, TM6SF2, PRR14L, ZIC5, SLC4A7, GORAB, PCDH18, VPS29, FAM178A, CEP170, NAT8, TMOD2, RAB11FIP1, PSEN1, CDKL4, AKAP13, TACC3, ADAM9, ZNF136, RAB9B, CYorf15B, POMC, C17orf101, CCNG1, AEBP2, H2AFY2, NFXL1, RPS6KA6, BTC, FAM108B1, CGNL1, DAZ1, DAZ3, DAZ2, DAZ4, C4orf3, ARSB, SPINLW1-WFDC6, NETO2, DCUN1D5, STON1, C9orf72, CAV2, IL6ST, CADPS2, C3orf25, NADK, SFTPA1, POU3F4, DSE, EIF3A, UPF3A, TTC9C, KIF18A, FAM101B, DAZL, GTPBP3, KLLN, NRSN2, GPSM2, TIA1, GRAMD3, UBC, PPAP2B, SPDYE3, UBASH3B, MYO1B, POU4F1, MDFIC, PRDM10, SESTD1, TMEM85, ZNF439, DCX, SLC19A3, PHACTR4, ZNF780B, HOOK1, CENPO, BCL7A, SLC35D3, IER3IP1, VAMP4, SEC61G, TAF2, SLCO1C1, KRTAP4-8, ARPP19, PRRC2B, CHRM5, PDC, ARPC5, SLC22A23, RDH12, LOC147670, C5orf42, CREBZF, TACSTD2, BIVM, TRAM1L1, NDFIP2, TRIM58, DDX4, POPDC3, RASGRP3, BTG1, TRMT1L, PAK3, KRTAP1-3, C10orf12, LOC100289187, MYLK3, FAM57A, ATAT1, PCDHB4, TDRD6, RICTOR, FAM13B, SLC7A1, MYO5C, KIAA1377, MED1, SEC63, ERMN, ANKRD13C, SPDYE5, ODZ1, IREB2, SPDYE1, SPDYE6, SETD4, KLHL8, SRD5A3, SERINC1, AIM1, MICAL3, DENND2C, MUC15, BTN3A1, MMP1, LGI1, C1GALT1, PARK2, SERPIND1
	hsa-miR-23a-3p	RING1, CXCL12, HES1, POU4F2, Celf1, ATAT1, IL6R, PPARGC1A, G6PC, FOXO3, FANCG, MYH1, MYH2, MYH4, PTEN, PTPN11, HMGN2, ZNF117, ZNF138, ZNF208, ZNF493, ZNF107, ZNF676, ZNF626, KIAA1467, ZNF257, ZNF680, CARD8, ZNF765, MBOAT7, ZNF721, WBP2, PDE4B, ZIC4, MRC1, AUH, ZNF267, C2orf69, PNRC2, ALG6, CNOT4, MAK16, INTU, DEPDC1, FYB, ZNF254, SYT4, ZNF701, COG3, SCG5, TOP1, RUFY2, GPR155, POU4F2, PKP4, SLC6A14, TMEM68, SEMA6D, C3orf52, ZNF816-ZNF321P, ZNF732, ZNF761, PDE7A, PPP4R4, RAB8B, CDC40, CRISPLD1, LIN54, PCMTD2, RALYL, ZNF287, TMOD2, TMED5, FUT9, ZNF253, RGS18, RPL31, MTHFS, ST20-MTHFS, ZNF91, TMPO, MYCT1, ZNF30, ZNF100, CXCL12, USP51, DOCK3, RAB39B, ZNF708, NAP1L5, ZNF506, TMEM33, CTCF, MYH4, SATB1, C13orf34, TBC1D24, EMR2, PRPH2, TXLNG, CAB39, TNRC6A, SMN1, SMN2, SETD8, NEK6, PRKRIR, SLC38A2, SEC14L1, RAD51AP1, CNTLN, SERINC1, NUP50, RBM25, ATP6V1E1, HNF4G, TRAPPC6B, GLB1L3, PAH, SNRPG, KLF3, CYorf15B, UBL3, LOC100130932, ZNF395, APAF1, DPY19L4, SST, PPARGC1A, USP53, SEC23A, QSER1, FBXO32, EXOC3L4, ACSS3, VCAN, SPG20, SV2B, COL4A4, THUMPD3, PRLR, ZNF420, SEC23IP, C1orf96, ITGAL, CDC23, NACC2, GABRG1, ZNF28, RNF168, EFHA2, ABCC5, SNX5, AMBRA1, TBC1D12, C9orf5, TLK1, SLC12A1, ZNF780B, HEXIM1, CNOT6L, CLEC12B, LPHN2, LYZ, AUTS2, MTF1, SLC38A1, ZNF90, RNF38, ZBTB34, PNMA2, ARHGAP20, TNFAIP3, ALDH1A2, TPST1, HPGD, PIGX, ANKRD33B, ANKHD1, NLGN4X, CHUK, UBE2R2, ZDBF2, FGD4, DDX47, TADA1, CCNH, ZNF114, TRIM14, MAP7, FAS, IGSF8, TJP1, EXOC1, F2R, MT2A, PCDH18, GPRASP1, C13orf27, UTP23, ZDHHC21, MCM4, MAGEA5, MAGEA10-MAGEA5, C15orf32, LRAT, SLMO2, NFX1, FAM120AOS, DCLRE1A, CLDN12, SEC24A, SMPX, FILIP1, B4GALT4, PRDM10, KPNA4
	mml-miR-767-5p	

Table 7

Biological processes enriched by target genes of miRs that were increased or decreased in THC/SIV compared to VEH/SIV striatum

Category	miRs	Biological process of target genes	No. of genes
Decreased miR expression due to THC/SIV compared to VEH/SIV	mml-miR-338-5p_R-1 mml-let-7a-5p hsa-miR-151b_R+3 hsa-miR-181a-2-3p hsa-miR-151b_R+2 mml-miR-584-5p_R-1 mml-miR-211 mml-miR-15b-5p mml-miR-500a-3p	Regulation of transcription, DNA-dependent (86), from RNA polymerase II (69)	155
		Response to drug (22), hypoxia (15), estradiol (12), organic compounds (10), testosterone (5), glucocorticoid (4), nutrient levels (4), lipopolysaccharide (3)	75
		Signal transduction	54
		Apoptotic process	33
		Regulation of cell proliferation	47
		Receptor signaling, NGF (15), Insulin (12), MAPK (11), TGF (9)	47
		Cell cycle	42
		Blood coagulation	25
		Cell adhesion	25
		Protein phosphorylation	21
		Ubiquitin-dependent protein catabolic process	12
		Anterior/posterior pattern specification	9
		Response to wounding	8
		Regulation of translation	8
		Positive regulation of angiogenesis	5
		Astrocyte development	4
		Aging	4
		Inflammatory response	4
Increased miR expression due to THC/SIV compared to VEH/SIV	mml-miR-7_R+1 hsa-miR-137 hsa-miR-488-5p_R+2 mml-miR-628-5p mml-miR-299-3p hsa-miR-105-5p hsa-miR-488-3p hsa-miR-23a-3p mml-miR-767-5p	Regulation of transcription, DNA-dependent (57), from RNA polymerase II (59)	116
		Signal transduction	41
		Multicellular organismal development	36
		Receptor signaling EGF (8), insulin (5) LPS (4), ERK (4), NF-kappa B (4), MAPK (4)	29
		Apoptotic process	27
		Nervous system development	26
		Cell adhesion	25
		Protein transport	24
		Positive regulation of cell proliferation	19
		Interspecies interaction between organisms	18
		Negative regulation of cell proliferation	18
		Chromatin modification	14
		Negative regulation of protein phosphorylation	7
		Response to LPS (3), glucocorticoid (3)	6

Category	miRs	Biological process of target genes	No. of genes
		B cell differentiation	6
		Cell morphois	4
		Positive regulation of smooth muscle cell migration	4
		Protein stabilization	3
		Cell growth	3